

Supporting Information

Volatile Organic Compound Emissions from a Multi-Unit Residential Building to Ambient Air

Amirashkan Askari ^a, Arthur W.H. Chan ^{a,*}

^a Department of Chemical Engineering and Applied Chemistry, University of Toronto, Toronto, Canada, M5S 3E5

* corresponding author: arthurwh.chan@utoronto.ca

Table of contents

S1. Air sampling details.....	2
S1.1 Sampling apparatus.....	2
S1.2 Sampling procedure.....	2
S1.3 Ambient air condition during sampling.....	3
S2. Chemical analysis.....	5
S2.1 Instrumental analysis details.....	5
S2.2 Sample quantification.....	6
S2.3 Calibration and quality control/quality assurance.....	9
S3. Species concentration profiles.....	10
S4. VCP emissions in association with the sampling results.....	17
S4.1 Primary VCP sources associated with detected species.....	17
S4.2 Estimating VCP emissions from the sampling site building.....	19
S5. Building emissions influenced by indoor sources.....	19
S5.1 Indoor sinks strength compared to the air exchange rate.....	19
S5.2 MAU material balance.....	21
S6. Source apportionment analysis.....	24
S7. More discussion on the calculated indoor concentrations.....	27
S8. Proper statistical hypothesis tests to inspect significant trends across data.....	31
References.....	32

S1 Air sampling details

S1.1 Sampling apparatus

Figure S1 shows a schematic diagram of the sampling apparatus with the makeup air unit (MAU). Two assembled systems were employed in parallel to sample the air gas phase from MAU's inlet and exhaust streams. Each system actively pulled air through an adsorbent tube filled with TENAX®TA using an air pump.

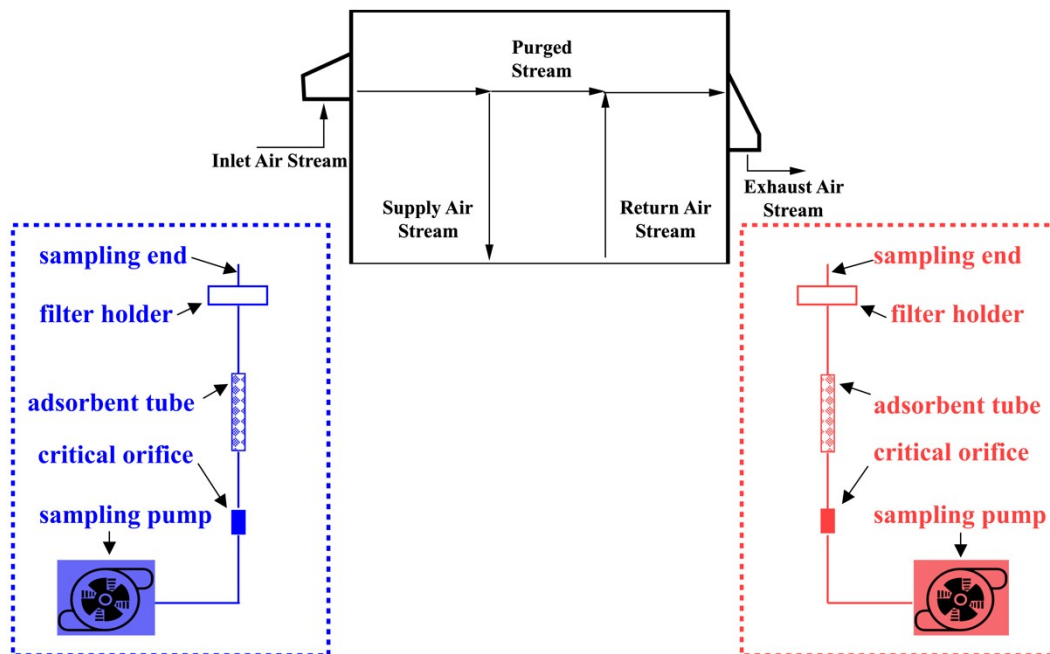


Figure S1- sampling apparatus associated with exhaust and inlet air streams of the makeup air unit (MAU).

A filter holder housing a 47-mm quartz filter laced with 20% (w/w) aqueous sodium thiosulfate solution was installed between the sampling end and the adsorbent tube to stop airborne particles from entering the adsorbent tube (Figure S1). Sodium thiosulfate on the filter removed ozone to protect the adsorbed species downstream from ozonolysis. The filters were submerged in the sodium thiosulfate solution overnight and were perfectly dried under a stream of nitrogen before being loaded into the sampling setup. A critical orifice was installed between the air pump and the adsorbent tube to keep the sampling flow rate below $150 \text{ mL}\cdot\text{min}^{-1}$. Higher flow rates may cause adsorbate breakthroughs from the adsorbent tube or reduce adsorption efficiency because of the decreased interaction time between the gas and solid phase. All sampling tubing was made of air sampling-grade Teflon lines, assembled using Swagelok connections.

S1.2 Sampling procedure

Before each sampling session, eleven TENAX®TA adsorbent tubes (Gerstel GmbH & Ko. KG, Germany) were conditioned under helium flow at 320°C for fifty minutes. Eight tubes were selected for air sampling, four for inlet data, and four for exhaust. Two tubes were shipped to the sampling site as field blanks. The last tube was kept as an analytical blank. The adsorbent tubes were identified by codes printed on their body. Tube selection for sampling or blank measurements was conducted randomly to avoid biases associated with specific adsorbent tubes. All eleven tubes

were spiked with 1 μL of a 10 $\text{ng}/\mu\text{L}$ solution of deuterated toluene in methanol, hereafter designated as the internal standard. As discussed in Section S2, the internal standard tracked the instrument sensitivity variation across sample runs. Furthermore, the internal standard ratio between a sample/field blank and the analytical blank was used to infer species recovery ratios. The analytical blank tube was analyzed immediately after the tube spiked with the internal standard solution. The conditioned tubes were capped with Teflon stoppers and shipped to the field in a cooler box filled with Cold Bricks (ULINE, USA).

During the field measurements, the tubes selected for sampling were taken out of the cold preserving box just before the sampling time and were capped and stored back in the box immediately after sampling. Air flow rates were measured at the beginning and the end of each sampling round using a Gilibrator-2 flow calibrator (Sensidyne, USA). The sampled volume was calculated from Equation S1.

$$V_{\text{sample}} = \left(\frac{F_{\text{beg}} + F_{\text{end}}}{2} \right) \times \Delta t_{\text{sample}} \quad \text{S1}$$

In Equation S1, V_{sample} is the sampled air volume (L). F_{beg} and F_{end} designate the sampling flow rates ($\text{L}\cdot\text{min}^{-1}$) at the beginning and the end of sampling, respectively. Δt_{sample} refers to sampling duration (min).

The field blank tubes were uncapped and loaded into the sampling setup for thirty seconds at the sampling site while the air pumps were turned off. All the samples and field blanks were returned to the lab and analyzed within 24 hours.

S1.3 Ambient air condition during sampling

Weather condition was logged during the sampling campaign, including ambient temperature, pressure, relative humidity, wind speed, and wind direction. The weather parameters were taken from Billy Bishop Toronto City Airport meteorology station.¹ As discussed in Section B.2, ambient temperature and pressure are used to calculate Normal Volumes of sampled air. Figure S2 shows temperature, pressure, and relative humidity distribution throughout the campaign's four sampling time intervals. Figure S2 demonstrates that temperatures were between -10°C and 5°C , with mean values of about 2°C . Ambient pressure means were slightly below 101 kPa, and relative humidity varied from about 50% to 90%, with average values within 65% to 70%. In addition to temperature data taken from the airport meteorology station, the temperature of the exhaust stream was measured four times during each sampling round using a mercury thermometer held for two minutes exposed to the exhaust stream. The exhaust stream temperatures were consistent during the campaign, with an average of 15°C and a standard deviation of about 1°C .

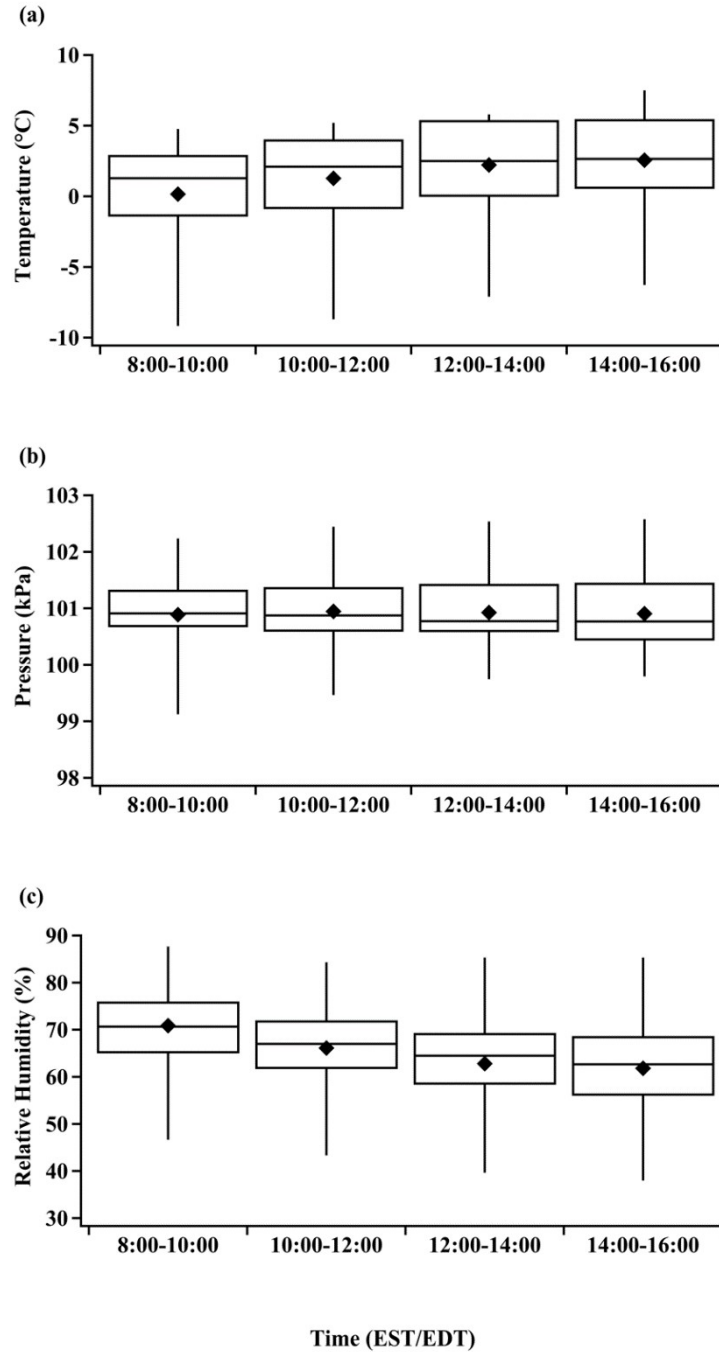


Figure S2- ambient weather conditions at the measurement site during the air sampling campaign. (a) ambient temperature (°C), (b) ambient pressure (kPa), and (c) relative air humidity.

Figure S3 shows the wind roses associated with the sampling dates. The sampling site was more frequently downwind of northwestern winds. These winds can bring car and train emissions from the Gardiner Expressway and the Canada National Railway to the sampling site, although these routes are closer to the site from the Northeast direction (See Figure 1 of the main text). Winds from southeast to southwest, where the Billy Bishop Airport is located, were less frequent. Thus, the ambient data were less likely to be influenced by airport emissions.

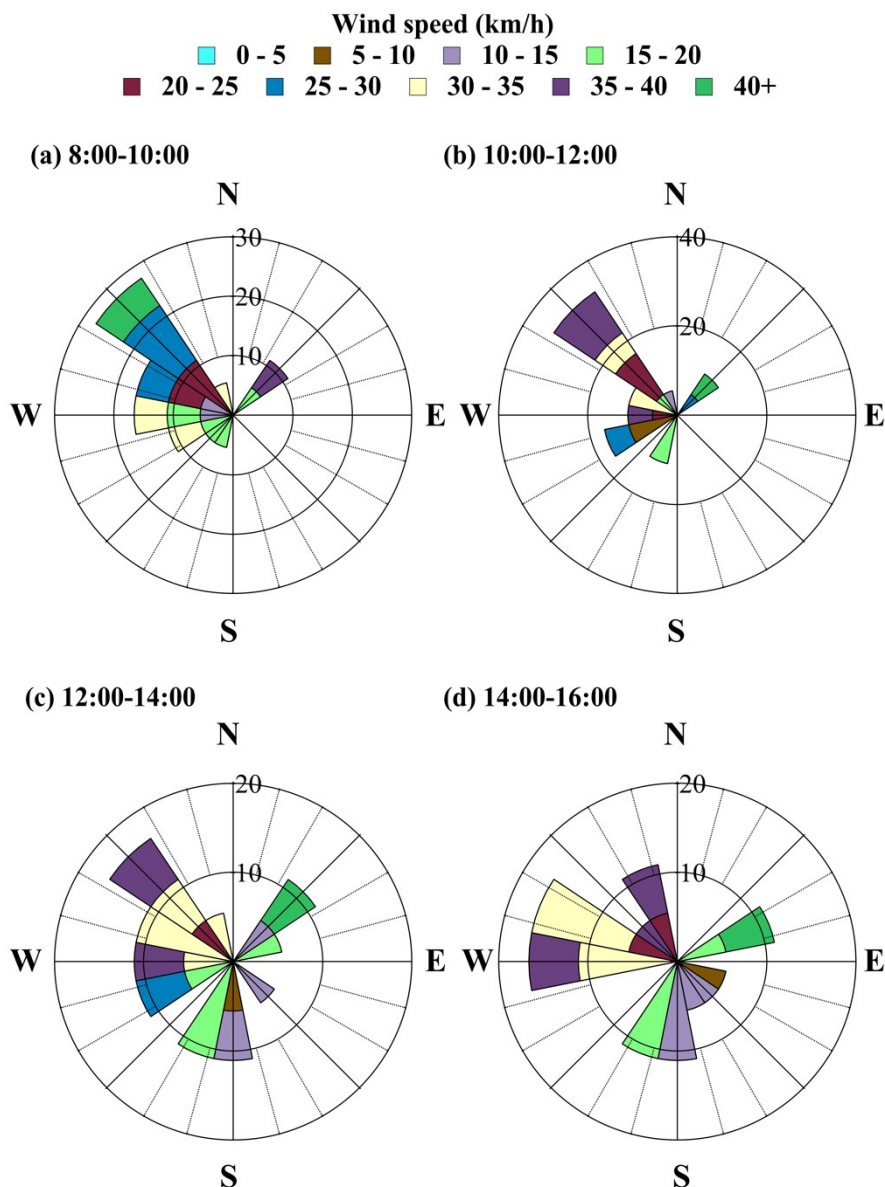


Figure S3- wind roses demonstrating wind speed (km/h) and direction during various time intervals throughout the air sampling campaign.

S2 Chemical analysis

S2.1 Instrumental analysis details

The samples were analyzed using thermal desorption-gas chromatography/mass spectrometry (TD-GC/MS). The thermal desorption system (Gerstel GmbH & Ko. KG, Germany) increased the adsorbent tube temperature from 50°C to 300°C with a 60°C.min⁻¹ ramp. During desorption, the desorbed species were focused on a cold trap involving a cartridge filled with TANAX®TA, which was kept at -15°C by intermittent liquid nitrogen injection into the cold injection system (CIS) housing the trap. Upon the completion of the desorption cycle, the CIS temperature increased to 320°C with a 12°C.min⁻¹ temperature ramp, desorbing the trapped species. Species desorbed from CIS were injected into the gas chromatograph in a split-less mode.

The gas chromatograph (GC 7980B, Agilent, USA) utilized a non-polar Rtx®-5MS column (Restek, USA). The nominal column dimensions were 30 m x 250 µm x 1 µm (length x outer diameter x stationary phase thickness). Helium carrier gas flowed with a rate of 1 mL.min⁻¹ through the column. The temperature program of the chromatographic analysis involved holding an initial temperature of 35°C for two minutes, then warming the GC oven to 320°C with a temperature ramp of 10°C.min⁻¹. The GC-MS interface was kept at 250°C during the analysis. The mass spectrometer (MS 5977A, Agilent, USA) employed the electron impact (EI) ionization mode, powered by an electromagnetic voltage of 1390 V. The ionized species were processed by a quadrupole scanner, with a frequency of 3.1 scans.second⁻¹. The scanning covered mass-to-charge ratio (*m/z*) values from 30 to 500 with a 0.1 step size. The ion source started functioning after two minutes following the start of the chromatographic analysis. During the analysis, the ion source and the quadrupole scanner were maintained at 230°C and 150°C, respectively.

S2.2 Sample quantification

The GC-MS results were analyzed using the MassHunter WorkStation – Qualitative Analysis software (Agilent, USA). The primary visual medium provided by the software out of data analysis is a total ion chromatogram (*TIC*), a plot of total mass-sensitive detected signal versus the chromatographic retention time. *TIC* signals are the sum of the detected signals of all mass-to-charge ratio (*m/z*) values. The software allows one to re-plot the chromatogram based on a given *m/z* signal to minimize the interference from species irrelevant to the analyte of interest. This modified chromatogram is known as an extracted ion chromatogram (*EIC*). We assumed the area under the extracted ion chromatogram around a given retention time to represent the analyte mass. The *EIC* areas were scaled by division to the *EIC* of the internal standard to account for instrument variability across different runs (See Equation S2).

$$m_i \sim \frac{EIC((m/z)_i, rt_i)}{EIC(m/z = 98, rt = 7.5 \text{ min})} = \hat{EIC}((m/z)_i, rt_i) \quad \text{S2}$$

In Equation S2, m_i is the mass of analyte i in nanograms. $EIC((m/z)_i, rt_i)$ is the area under the chromatogram extracted for an analyte-specific (See below) mass to charge ratio ($(m/z)_i$) and retention time (rt_i). The internal standard signal associated with deuterated toluene analysis is robust for the extracted ion chromatogram at $m/z = 98$ and $rt = 7.5 \text{ min}$. The dimensionless value from dividing the extracted ion chromatogram area of the analyte to the internal standard is designated as reduced EIC area ($\hat{EIC}((m/z)_i, rt_i)$) per the right-hand-side of Equation S2.

We determined the list of the chemical species of interest for detailed quantification following an initial untargeted analysis. 30% of the sample chromatograms were selected randomly and analyzed qualitatively to inspect species occurrence. The *TIC* mass spectra were reviewed every five seconds of retention time. The evolving *m/z* signals were identified as potential signifiers of a species occurrence. The potential mass spectrum was input into the NIST spectral library software (NIST, USA). The software evaluates the similarity between the input spectrum and the recorded spectra in its database based on match scores. Generally, a match score of 950 or above signifies robust similarity, while match scores below 700 indicate a poor parity. We selected species identifications with a match score above 800 for further examination. The retention times for the suspected species were converted to *n*-alkane retention indices (See Van Den Dool and Kratz²) and compared with the retention index records of the NIST Chemistry WebBook.³ The

NIST speciation was confirmed if the calculated retention index agreed with the recorded values by 10%. The abovementioned untargeted speciation scheme yielded 83 to 181 species identifications across the examined chromatograms. Fifty-two common species across at least two examined series were selected for targeted analysis for the next steps. Table S1 lists the species selected for targeted analysis.

Overall, in this study, species identification was based on both m/z and retention time, ensuring proper differentiation where possible. In cases where GC co-elution occurred, only compounds with sufficiently distinct spectral features and retention characteristics were quantified. Note that instances of unresolved co-elution represent a known limitation of single-stage GC-MS and would require tandem GC-MS or other advanced techniques for full separation.

Table S1- list of species selected for targeted analysis during this sampling campaign along with their associated effective saturation concentration (C^*), chemical formula, m/z , and retention index values associated with their extracted ion chromatograms *EICs*. The monoterpenoids associated with Figure 3 of the main text are printed in green.

species	Chemical formula	log C^* ^a	CAS number	m/z related to <i>EIC</i>	n -alkane retention index ^b
ethanol	CH ₃ CH ₂ OH	8.7	64-17-5	31	429 ± 12 ^c
isopropanol	(CH ₃) ₂ CHOH	8.9	67-63-0	45	500 ± 11
dichloromethane	CH ₂ Cl ₂	11.3	75-09-2	49	534 ± 9
methyl acetate	CH ₃ COOCH ₃	9.3	79-20-9	74	536 ± 10
methyl ethyl ketone (MEK)	CH ₃ C(O)CH ₂ CH ₃	9.1	78-93-3	43	599 ± 5
<i>n</i> -hexane	C ₆ H ₁₄	9.2	110-54-3	56	600 ± 0 ^d
ethyl acetate	CH ₃ CO ₂ CH ₂ CH ₃	8.3	141-78-6	43	616 ± 12
methylchloroform	CH ₃ CCl ₃	10.5	71-55-6	97	650 ± 5
cyclohexane	C ₆ H ₁₂	9.2	110-82-7	56	653 ± 17
1-butanol	C ₄ H ₉ OH	7.9	71-36-3	56	664 ± 3
methyl isobutyl ketone (MIBK)	(CH ₃) ₂ CHCH ₂ C(O)CH ₃	8.3	108-10-1	43	694 ± 5
<i>n</i> -heptane	C ₇ H ₁₆	8.8	142-82-5	57	700 ± 0 ^d
ethylene glycol monoethyl ether (EGEE)	CH ₃ CH ₂ OCH ₂ CH ₂ OH	6.0	110-80-5	59	716 ± 6
propylene glycol	CH ₃ CH(OH)CH ₂ OH	6.1	57-55-6	45	741 ± 11
2-methylheptane	C ₈ H ₁₈	8.4	592-27-8	43	766 ± 18
toluene	C ₆ H ₅ CH ₃	8.1	108-88-3	91	774 ± 4
<i>n</i> -octane	C ₈ H ₁₈	8.4	111-65-9	85	800 ± 0 ^d
<i>n</i> -butyl acetate	CH ₃ CO ₂ (CH ₂) ₃ CH ₃	8.0	123-86-4	43	814 ± 10
tetrachloroethylene	C ₂ Cl ₄	10.8	127-18-4	166	819 ± 6
2-methyloctane	C ₉ H ₂₀	7.9	3221-61-2	43	865 ± 17
ethylbenzene	C ₆ H ₅ CH ₂ CH ₃	7.7	100-41-4	91	871 ± 5

<i>m</i> & <i>p</i> -xylene	$(\text{CH}_3)_2\text{C}_6\text{H}_4$	7.7	108-38-3	91	878 ± 5
<i>n</i> -nonane	C_9H_{20}	7.9	111-84-2	57	900 ± 0 ^d
<i>o</i> -xylene	$(\text{CH}_3)_2\text{C}_6\text{H}_4$	7.7	95-47-6	91	906 ± 7
ethylene glycol monobutyl ether (EGBE)	$\text{CH}_3\text{CH}_2\text{CH}_2\text{CH}_2\text{-OC}_2\text{H}_4\text{OH}$	6.3	111-76-2	57	910 ± 7
C13 cycloalkanes	$\text{C}_{14}\text{H}_{28}$	5.8	1795-15-9	83	934 ± 14
α -thujene	$\text{CH}_2\text{CHC}(\text{CH}_3)\text{CHC}(\text{CH}_2)(\text{CHCH}_3\text{CH}_3)$	7.3	2867-05-2	93	937 ± 6
isopropylcyclohexane	$\text{C}_6\text{H}_{11}(\text{CHCH}_3\text{CH}_3)$	7.9	696-29-7	83	943 ± 8
α -pinene	$\text{C}_6\text{H}_7(\text{CH}_3)(\text{C}(\text{CH}_3)\text{CH}_3)$	7.4	7785-70-8	93	949 ± 4
2-methylnonane	$\text{C}_{10}\text{H}_{22}$	7.9	871-83-0	43	966 ± 9
octamethylcyclotetrasiloxane (D4)	$\text{Si}_4\text{O}_4(\text{CH}_3)_8$	5.7	556-67-2	281	984 ± 6
camphene	$\text{C}_6\text{H}_6(\text{CH}_3)_2(\text{CH}_2)$	7.4	28634-89-1	93	988 ± 9
β -pinene	$\text{C}_6\text{H}_6(\text{CH}_2)(\text{CH}_3)_2$	7.4	127-91-3	93	996 ± 5
<i>n</i> -decane	$\text{C}_{10}\text{H}_{22}$	7.5	124-18-5	57	1000 ± 0 ^d
1,2,4-trimethylbenzene	$\text{C}_6\text{H}_3(\text{CH}_3)_3$	7.3	95-63-6	105	1007 ± 14
β -ocimene	$\text{CH}_3\text{C}(\text{CH}_3)\text{C}_3\text{H}_4(\text{CH}_3)\text{C}_2\text{H}_3$	7.2	13877-91-3	93	1027 ± 11
D-limonene	$\text{C}_6\text{H}_8(\text{CH}_3)(\text{C}(\text{CH}_3)\text{CH}_2)$	7.3	138-86-3	68	1043 ± 3
eucalyptol	$\text{C}_6\text{H}_{10}(\text{CH}_3)(\text{OC}(\text{CH}_3)\text{CH}_3)$	6.8	470-82-6	93	1050 ± 3
2-methyldecane	$\text{C}_{11}\text{H}_{24}$	7.1	6975-98-0	57	1063 ± 6
3-carene	$\text{C}_6\text{H}_7(\text{CH}_3)(\text{C}(\text{CH}_3)\text{CH}_3)$	7.4	13466-78-9	93	1073 ± 5
<i>n</i> -undecane	$\text{C}_{11}\text{H}_{24}$	7.1	1120-21-4	57	1100 ± 0 ^d
linalool	$\text{C}_2\text{H}_3\text{C}(\text{CH}_3)(\text{OH})\text{C}_3\text{H}_5\text{C}(\text{CH}_3)\text{CH}_3$	5.1	78-70-6	93	1107 ± 6
decamethylcyclopentasiloxane (D5)	$\text{Si}_5\text{O}_5(\text{CH}_3)_{10}$	4.0	541-02-6	355	1066 ± 5
camphor	$\text{C}_5\text{H}_7\text{O}(\text{CH}_3)(\text{C}(\text{CH}_3)\text{CH}_3)$	6.5	464-48-2	93	1175 ± 9
<i>n</i> -dodecane	$\text{C}_{12}\text{H}_{26}$	6.7	112-40-3	57	1200 ± 0 ^d
phenoxyethanol	$\text{C}_6\text{H}_5\text{OC}_2\text{H}_4\text{OH}$	4.5	122-99-6	94	1240 ± 5
1-phenoxy-2-propanol	$\text{C}_6\text{H}_5\text{OCH}(\text{OH})\text{CH}_3$	4.1	770-35-4	94	1264 ± 7
<i>n</i> -tridecane	$\text{C}_{13}\text{H}_{28}$	6.2	629-50-5	57	1300 ± 0 ^d
<i>n</i> -tetradecane	$\text{C}_{14}\text{H}_{30}$	5.8	629-59-4	57	1400 ± 0 ^d
<i>n</i> -pentadecane	$\text{C}_{15}\text{H}_{32}$	5.4	629-62-9	57	1500 ± 0 ^d

^a log C* values were estimated using the SIMPOL 1.0 method.⁴

^b The retention indices are listed as average \pm standard deviation based on all analysis results.

^c Our sampling setup could not detect *n*-butane, impeding the experimental determination of *n*-alkane retention index for ethanol. The value indexed in the table was taken from chromatographic analysis conditions similar to this study from NIST Chemistry Webbook.³

^d An *n*-alkane is assumed to have a retention index of $(100 \times n)$ with perfect precision (i.e., standard deviation = 0).

The analyte mass within samples was identified by converting the reduced *EIC* area, as given by Equation S2, of the species of interest to the equivalent value for the closest normal alkane in retention time (See Equation S3). For example, if the analyte's retention time lies between *n*-octane and *n*-nonane, and the analyte's retention time is closer to that of *n*-octane, the reduced *EIC* will be converted to *n*-octane equivalent.

$$EIC_{alkane,eq}((m/z)_i, rt_i) = EIC((m/z)_i, rt_i) \times \frac{f_{(m/z)_{alkane}}}{f_{(m/z)_i}} \quad S3$$

In Equation S3, $EIC_{alkane,eq}((m/z)_i, rt_i)$ is the normal alkane equivalent reduced *EIC* area for the analyte of interest. $f_{(m/z)_i}$ and $f_{(m/z)_{alkane}}$ are the fraction of the species mass spectrum signal accounted by the specific *m/z* of the species of interest and the surrogating alkane, respectively (See the second column of Table S1). The $EIC_{alkane,eq}((m/z)_i, rt_i)$ is readily converted to analyte mass using the alkane calibration curve equation (See Table S2). This quantification method implies that the instrument response and sensitivity stays invariant across the analytes and their normal alkane equivalents. We assume this applies to a good approximation for most species listed in Table S1. Cyclic siloxanes were excluded from this method since their molecular structure is pretty different from normal alkanes. The instrument was separately calibrated for octamethylcyclotetrasiloxane (D4) and decamethylcyclopentasiloxane (D5).

Table S2- calibration curve parameters (slope and intercept) for the normal alkanes used for external calibration. The calibration curves yield analyte mass in nanograms as a dependent variable on the *EIC* normal alkane equivalent reduced area (See Equation S2). The slope and intercept variability ranges correspond to 95% confidence intervals.

species	Chemical formula	<i>m/z</i> related to <i>EIC</i>	calibration line slope	calibration line intercept
<i>n</i> -hexane	C ₆ H ₁₄	86	632.61 \pm 40.11	3.20 \pm 1.05
<i>n</i> -heptane	C ₇ H ₁₆	43	20.07 \pm 2.15	2.22 \pm 0.98
<i>n</i> -octane	C ₈ H ₁₈	43	7.31 \pm 0.67	2.10 \pm 0.76
<i>n</i> -nonane	C ₉ H ₂₀	57	6.61 \pm 0.51	1.84 \pm 0.09
<i>n</i> -decane	C ₁₀ H ₂₂	57	5.22 \pm 0.42	0.25 \pm 0.02
<i>n</i> -undecane	C ₁₁ H ₂₄	57	4.80 \pm 0.31	-0.63 \pm 0.03
<i>n</i> -dodecane	C ₁₂ H ₂₆	57	4.79 \pm 0.39	-0.49 \pm 0.03
<i>n</i> -tridecane	C ₁₃ H ₂₈	57	4.73 \pm 0.36	-0.84 \pm 0.05
<i>n</i> -tetradecane	C ₁₄ H ₃₀	57	4.67 \pm 0.32	-0.43 \pm 0.08
<i>n</i> -pentadecane	C ₁₅ H ₃₂	57	4.72 \pm 0.29	-0.69 \pm 0.13
<i>n</i> -hexadecane	C ₁₆ H ₃₄	57	4.92 \pm 0.34	-0.62 \pm 0.04
<i>n</i> -heptadecane	C ₁₇ H ₃₆	57	4.51 \pm 0.23	-0.12 \pm 0.01
<i>n</i> -octadecane	C ₁₈ H ₃₈	57	3.59 \pm 0.31	0.87 \pm 0.04
<i>n</i> -nonadecane	C ₁₉ H ₄₀	57	4.67 \pm 0.25	-0.13 \pm 0.05

A fraction of the sampled analyte may be lost from the adsorbent tube before analysis. The ratio of the internal standard chromatographic area (i.e., $EIC(m/z = 98, rt = 7.5 \text{ min})$) between the sample data and the analytical blank was used to scale the quantified mass to account for possible analyte losses (Equation S4).

$$m_i = m_{i,quantified} \times \frac{EIC(m/z = 98, rt = 7.5 \text{ min})_{AB}}{EIC(m/z = 98, rt = 7.5 \text{ min})_{sample}} \quad S4$$

In Equation S4, $m_{i,quantified}$ is the analyte mass found from the normal alkane calibration curve as discussed in Section S2.3. m_i is the scaled analyte mass based on the internal standard signal ratio between the analytical blank (AB) and the sample.

Species Normal concentrations were calculated by dividing the quantified mass by the sampled volume, as given by Equation S1. The original sample volumes were converted to normal volumes (i.e., air volume at 20°C and 1 atm) using the ideal gas law to make a consistent framework for further discussion on concentration values (Equation S5).

$$C_i = \frac{m_i}{V_{sample}} \times \frac{T_{sample}}{T_{normal} = 293.15K} \times \frac{P_{normal} = 101.325 \text{ kPa}}{P_{sample}} \quad S5$$

In Equation S5, T_{sample} and P_{sample} are air temperature and pressure during the sampling in Kelvins and kilopascals, respectively (See Figure S2). C_i is the species normal concentration ($\frac{\mu g}{m^3}$).

S2.3 Calibration and quality control/quality assurance

Instrument calibration was achieved by running different concentrations of external standards of C6 to C19 normal alkanes (AccuStandard, USA). Calibration standards were prepared by dissolving normal alkanes in methanol. Normal alkanes within the volatility range of C6 to C15 were directly dissolved in methanol, while the less volatile ones were first transferred into the liquid phase by preparing 10% w/w solutions in ethylbenzene. The chromatographic analysis of the external standards with concentrations of 100, 75, 50, 25, 10, 5, 2.5, and 1 ng·μL⁻¹ of normal alkanes in methanol was carried out. One microliter of each solution was injected directly into the adsorbent tube. The adsorbent tubes were also spiked with one microliter of the analytical standard and were subsequently analyzed by TD-GC/MS. The calibration curves were characterized as linear interpolations of analyte mass in nanograms versus the reduced EIC area (See Section S2.2). In addition to the abovementioned eight non-zero concentrations, each calibration batch involved an analytical blank prepared by spiking the adsorption tube only with 1 μL of the internal standard. The analytical blank results were added as 0 ng·μL⁻¹ data points to the calibration set. Instrument calibration was repeated eleven times during the sampling campaign. The instrument response was reproducible with less than 10% calibration data variations (See slope and intercept uncertainties in Table S2).

The analyte limit of detection (LOD) was determined in association with $EIC_{LOD}((m/z)_i, RT_i)$ as given by Equation S6.

$$EIC_{LOD}((m/z)_i, RT_i) = Mean(EIC_{AB}((m/z)_i, rt_i)) + 3 \times Std(EIC_{FB}((m/z)_i, rt_i)) \quad S6$$

In Equation S6, $\hat{E}IC_{LOD}$, $\hat{E}IC_{AB}$, and $\hat{E}IC_{FB}$ denote reduced EIC areas for the LOD, analytical blanks, and field blanks, respectively. Equation S6 indicates that the LOD is calculated by adding three folds of the standard deviation (Std) of field blank data to the mean ($Mean$) of the analytical blanks. The $\hat{E}IC_{LOD}$ value is converted to equivalent LOD mass. LOD values are indexed in Table S3, Table S4, and Table S5. During sampling quantitation, any analytical mass smaller the LOD value was logged as below detection ($< LOD$).

S3 Species concentration profiles

Table S3 and Table S4 list the concentration distributions for exhaust and inlet samples, respectively. Table S5 involves the same data for calculated effective indoor concentrations (See Section S5.2). The numbers in Table S3, Table S4, and Table S5 result from aggregating bihourly-collected data. The more detailed database is uploaded on an online database on figshare (DOI: 10.6084/m9.figshare.24328816).

Table S3- concentration distribution information ($\mu\text{g}/\text{m}^3$) along with detection frequencies and limit of detection (LOD) values for MAU's exhaust data.

species	Chemical formula	detection frequency (%)	LOD (ng)	min ($\mu\text{g}/\text{m}^3$)	1 st quartile ($\mu\text{g}/\text{m}^3$)	median ($\mu\text{g}/\text{m}^3$)	3 rd quartile ($\mu\text{g}/\text{m}^3$)	max ($\mu\text{g}/\text{m}^3$)	mean ($\mu\text{g}/\text{m}^3$)
1-butanol	$\text{C}_4\text{H}_9\text{OH}$	98	0.198	< LOD	1.407	1.946	2.537	5.135	2.112
1-phenoxy-2-propanol	$\text{C}_6\text{H}_5\text{OCH}(\text{OH})\text{CH}_3$	59	0.001	< LOD	< LOD	0.006	0.015	0.033	0.009
1,2,4-trimethylbenzene	$\text{C}_6\text{H}_3(\text{CH}_3)_3$	93	0.004	0.000	0.027	0.031	0.042	0.087	0.035
2-methyldecane	$\text{C}_{11}\text{H}_{24}$	100	0.011	0.053	0.122	0.180	0.308	0.987	0.265
2-methylheptane	C_8H_{18}	23	0.371	< LOD	< LOD	< LOD	< LOD	0.486	< LOD
2-methylnonane	$\text{C}_{10}\text{H}_{22}$	89	0.004	< LOD	0.067	0.090	0.129	0.392	0.103
2-methyloctane	C_9H_{20}	95	0.006	< LOD	0.215	0.265	0.339	0.484	0.273
3-carene	$\text{C}_6\text{H}_7(\text{CH}_3)(\text{C}(\text{CH}_3)\text{CH}_3)$	79	0.011	< LOD	0.012	0.027	0.045	0.155	0.037
<i>n</i> -butyl acetate	$\text{CH}_3\text{CO}_2(\text{CH}_2)_3\text{CH}_3$	100	0.098	0.149	0.608	0.800	1.096	6.089	1.056
C13 cycloalkanes	$\text{C}_{14}\text{H}_{28}$	97	0.001	< LOD	0.118	0.127	0.137	0.179	0.126
camphene	$\text{C}_6\text{H}_6(\text{CH}_3)_2(\text{CH}_2)$	98	0.014	< LOD	0.048	0.064	0.094	0.129	0.070
camphor	$\text{C}_5\text{H}_7\text{O}(\text{CH}_3)(\text{C}(\text{CH}_3)\text{CH}_3)$	74	0.007	< LOD	< LOD	0.143	0.257	0.429	0.151
<i>D</i> -limonene	$\text{C}_6\text{H}_8(\text{CH}_3)(\text{C}(\text{CH}_3)\text{CH}_2)$	100	0.004	0.228	2.328	2.955	4.005	6.996	3.175
decamethylcyclopentasiloxane (D5)	$\text{Si}_5\text{O}_5(\text{CH}_3)_{10}$	100	0.046	0.262	2.156	3.344	4.365	7.743	3.341
ethanol	$\text{CH}_3\text{CH}_2\text{OH}$	100	0.001	0.847	3.584	5.110	6.517	11.171	5.169
ethyl acetate	$\text{CH}_3\text{CO}_2\text{CH}_2\text{CH}_3$	100	0.001	0.254	2.437	3.063	4.926	17.776	3.985
ethylbenzene	$\text{C}_6\text{H}_5\text{CH}_2\text{CH}_3$	95	0.085	< LOD	0.218	0.301	0.435	0.753	0.336
ethylene glycol monobutyl ether (EGBE)		97	0.054	< LOD	0.280	0.398	0.643	1.367	0.472
ethylene glycol monoethyl ether (EGEE)	$\text{CH}_3\text{CH}_2\text{OCH}_2\text{CH}_2\text{OH}$	100	0.004	0.170	0.923	1.598	3.455	11.704	2.298
eucalyptol	$\text{C}_6\text{H}_{10}(\text{CH}_3)(\text{OC}(\text{CH}_3)\text{CH}_3)$	100	0.004	0.043	0.175	0.223	0.487	13.201	1.062
isopropanol	$(\text{CH}_3)_2\text{CHOH}$	100	1.071	1.316	7.746	15.489	23.615	34.344	15.748
isopropylcyclohexane	$\text{C}_6\text{H}_{11}(\text{CHCH}_3\text{CH}_3)$	100	0.001	0.105	0.158	0.175	0.193	0.294	0.181
linalool	$\text{C}_2\text{H}_3\text{C}(\text{CH}_3)(\text{OH})\text{C}_3\text{H}_5\text{C}(\text{CH}_3)\text{CH}_3$	34	0.003	< LOD	< LOD	< LOD	0.012	0.067	0.010
<i>m</i> & <i>p</i> -xylene	$(\text{CH}_3)_2\text{C}_6\text{H}_4$	100	0.016	0.139	0.429	0.609	1.036	2.244	0.778
methyl acetate	$\text{CH}_3\text{COOCH}_3$	44	0.057	< LOD	< LOD	< LOD	0.296	0.544	0.147
methyl ethyl ketone (MEK)	$\text{CH}_3\text{C}(\text{O})\text{CH}_2\text{CH}_3$	98	0.331	< LOD	1.598	1.903	2.360	4.311	2.015

methyl isobutyl ketone (MIBK)	$(\text{CH}_3)_2\text{CHCH}_2\text{C}(\text{O})\text{CH}_3$	98	0.067	< LOD	0.701	0.850	1.147	5.652	1.098
<i>n</i> -decane	$\text{C}_{10}\text{H}_{22}$	> 99	0.108	< LOD	0.233	0.361	2.698	12.928	1.769
<i>n</i> -dodecane	$\text{C}_{12}\text{H}_{26}$	> 99	0.035	< LOD	0.108	0.152	0.223	0.843	0.192
<i>n</i> -heptane	C_7H_{16}	100	0.098	0.406	2.461	2.952	3.831	7.431	3.402
<i>n</i> -hexane	C_6H_{14}	100	0.065	0.428	1.093	1.404	1.891	3.226	1.486
<i>n</i> -nonane	C_9H_{20}	100	0.018	0.149	0.365	0.478	0.677	1.301	0.541
<i>n</i> -octane	C_8H_{18}	100	0.017	0.240	0.832	1.134	1.598	3.191	1.311
<i>n</i> -pentadecane	$\text{C}_{15}\text{H}_{32}$	28	0.124	< LOD	< LOD	< LOD	< LOD	0.274	< LOD
<i>n</i> -tetradecane	$\text{C}_{14}\text{H}_{30}$	98	0.020	< LOD	0.084	0.111	0.144	0.317	0.119
<i>n</i> -tridecane	$\text{C}_{13}\text{H}_{28}$	93	0.026	< LOD	0.045	0.062	0.075	0.188	0.062
<i>n</i> -undecane	$\text{C}_{11}\text{H}_{24}$	> 99	0.118	< LOD	0.192	0.285	0.490	2.565	0.446
<i>o</i> -xylene	$(\text{CH}_3)_2\text{C}_6\text{H}_4$	100	0.009	0.115	0.229	0.296	0.408	0.694	0.334
octamethylcyclotetrasiloxane (D4)	$\text{Si}_4\text{O}_4(\text{CH}_3)_8$	100	0.031	0.085	0.178	0.252	0.361	6.335	0.478
phenoxyethanol	$\text{C}_6\text{H}_5\text{OC}_2\text{H}_4\text{OH}$	84	0.006	< LOD	< LOD	0.010	0.020	0.052	0.013
propylene glycol	$\text{CH}_3\text{CH}(\text{OH})\text{CH}_2\text{OH}$	89	0.018	< LOD	0.425	0.615	0.810	1.760	0.634
tetrachloroethylene		100	0.004	0.116	0.192	0.213	0.286	0.857	0.252
toluene	$\text{C}_6\text{H}_5\text{CH}_3$	100	0.116	0.213	1.091	1.468	2.616	5.835	1.952
α -pinene	$\text{C}_6\text{H}_7(\text{CH}_3)(\text{C}(\text{CH}_3)\text{CH}_3)$	100	<	0.001	0.138	0.521	0.612	0.851	2.345
α -thujene	$\text{CH}_2\text{CHC}(\text{CH}_3)\text{CHC}(\text{CH}_2)(\text{CHCH}_3\text{CH}_3)$	98	<	0.005	< LOD	0.131	0.143	0.161	0.221
β -ocimene	$\text{CH}_3\text{C}(\text{CH}_3)\text{C}_3\text{H}_4(\text{CH}_3)\text{C}_2\text{H}_3$	100	<	0.001	0.021	0.096	0.123	0.154	0.317
β -pinene	$\text{C}_6\text{H}_6(\text{CH}_2)(\text{CH}_3)_2$	100	<	0.007	0.040	0.278	0.369	0.459	1.011

Table S4- concentration distribution information ($\mu\text{g}/\text{m}^3$) along with detection frequencies and limit of detection (LOD) values for MAU's inlet data.

species	Chemical formula	detection frequency (%)	LOD (ng)	min ($\mu\text{g}/\text{m}^3$)	1 st quartile ($\mu\text{g}/\text{m}^3$)	median ($\mu\text{g}/\text{m}^3$)	3 rd quartile ($\mu\text{g}/\text{m}^3$)	max ($\mu\text{g}/\text{m}^3$)	mean ($\mu\text{g}/\text{m}^3$)
1-butanol	$\text{C}_4\text{H}_9\text{OH}$	88	0.198	< LOD	0.805	1.049	1.398	4.675	1.140
1-phenoxy-2-propanol	$\text{C}_6\text{H}_5\text{OCH}(\text{OH})\text{CH}_3$	30	0.001	<	< LOD	< LOD	0.004	0.024	0.003
1,2,4-trimethylbenzene	$\text{C}_6\text{H}_3(\text{CH}_3)_3$	64	0.004	< LOD	< LOD	0.021	0.029	0.127	0.021
2-methyldecane	$\text{C}_{11}\text{H}_{24}$	67	0.011	< LOD	< LOD	0.021	0.045	0.147	0.029
2-methylnonane	$\text{C}_{10}\text{H}_{22}$	69	0.004	< LOD	< LOD	0.049	0.073	0.244	0.049
2-methyloctane	C_9H_{20}	96	0.006	< LOD	0.191	0.265	0.394	0.975	0.303

<i>n</i> -butyl acetate	CH ₃ CO ₂ (CH ₂) ₃ CH ₃	100	0.098 <	0.145 < LOD	0.275 < LOD	0.396 < LOD	0.645	8.302	0.676
C13 cycloalkanes	C ₁₄ H ₂₈	49	0.001				0.111	0.525	0.073
camphene	C ₆ H ₆ (CH ₃) ₂ (CH ₂)	27	0.014	< LOD	< LOD	< LOD	0.015	0.063	0.000
camphor	C ₅ H ₇ O(CH ₃)(C(CH ₃)CH ₃)	91	0.007	< LOD	0.053	0.107	0.183	0.381	0.128
<i>D</i> -limonene	C ₆ H ₈ (CH ₃)(C(CH ₃)CH ₂)	100	0.004	0.077	0.163	0.235	0.403	5.366	0.437
decamethylcyclopentasiloxane (D5)	Si ₅ O ₅ (CH ₃) ₁₀	> 99	0.046	< LOD	0.229	0.350	0.554	1.885	0.477
dichloromethane	CH ₂ Cl ₂ CH ₃ CH ₂ OH	6	4.451 <	< LOD	< LOD	< LOD	< LOD	17.037	< LOD
ethanol		82	0.001	< LOD	0.215	0.496	0.821	3.954	0.579
ethyl acetate	CH ₃ CO ₂ CH ₂ CH ₃		<						
ethylbenzene	CH ₃ CO ₂ CH ₂ CH ₃	97	0.001	< LOD	0.633	0.967	1.917	23.570	2.079
ethylene glycol monobutyl ether (EGBE)	C ₆ H ₅ CH ₂ CH ₃	97	0.085	< LOD	0.197	0.250	0.337	1.161	0.296
ethylene glycol monoethyl ether (EGEE)	CH ₃ CH ₂ CH ₂ CH ₂ - OC ₂ H ₄ OH	97	0.054	< LOD	0.254	0.433	0.623	1.310	0.461
eucalyptol	CH ₃ CH ₂ OCH ₂ CH ₂ OH	100	0.004	0.137	1.449	2.337	4.829	10.013	3.278
isopropanol	C ₆ H ₁₀ (CH ₃)(OC(CH ₃)CH ₃) (CH ₃) ₂ CHOH	99 85	0.004 1.071 <	< LOD < LOD	0.041 < LOD	0.059 1.690	0.114 5.504	13.689 39.588	0.639 4.852
isopropylcyclohexane	C ₆ H ₁₁ (CHCH ₃ CH ₃)	93	0.001	< LOD	0.114	0.134	0.168	0.562	0.151
<i>m</i> & <i>p</i> -xylene	(CH ₃) ₂ C ₆ H ₄	100	0.016	0.210	0.309	0.431	0.689	3.165	0.569
methyl ethyl ketone (MEK)	CH ₃ C(O)CH ₂ CH ₃	99	0.331	< LOD	1.338	1.725	2.502	5.720	2.074
methyl isobutyl ketone (MIBK)	(CH ₃) ₂ CHCH ₂ C(O)CH ₃	100	0.067	0.383	0.620	0.798	1.118	7.327	1.124
<i>n</i> -decane	C ₁₀ H ₂₂	96	0.108	< LOD	< LOD	< LOD	0.150	0.388	0.122
<i>n</i> -dodecane	C ₁₂ H ₂₆	76	0.035	< LOD	< LOD	< LOD	0.049	0.273	0.036
<i>n</i> -heptane	C ₇ H ₁₆	100	0.098	0.894	1.894	2.540	3.831	8.112	2.919
<i>n</i> -hexane	C ₆ H ₁₄	100	0.065	0.619	1.076	1.400	1.769	7.152	1.576
<i>n</i> -nonane	C ₉ H ₂₀	100	0.018	0.196	0.311	0.673	1.038	2.262	0.761
<i>n</i> -octane	C ₈ H ₁₈	100	0.017	0.464	0.848	1.208	2.612	5.513	1.819
<i>n</i> -pentadecane	C ₁₅ H ₃₂	81	0.124	< LOD	< LOD	< LOD	0.142	0.359	< LOD
<i>n</i> -tetradecane	C ₁₄ H ₃₀	67	0.020	< LOD	< LOD	< LOD	0.028	0.107	< LOD
<i>n</i> -tridecane	C ₁₃ H ₂₈	69	0.026	< LOD	< LOD	< LOD	0.032	0.074	< 0.001
<i>o</i> -xylene	(CH ₃) ₂ C ₆ H ₄	100	0.009	0.133	0.188	0.240	0.308	1.114	0.284
octamethylcyclotetrasiloxane (D4)	Si ₄ O ₄ (CH ₃) ₈	94	0.031	< LOD	0.091	0.149	0.235	0.606	0.165
Phenoxyethanol	C ₆ H ₅ OC ₂ H ₄ OH	40	0.006	< LOD	< LOD	< LOD	0.007	0.049	< LOD
propylene glycol	CH ₃ CH(OH)CH ₂ OH	99	0.018	< LOD	0.337	0.630	0.889	3.042	0.705

tetrachloroethylene	C ₂ Cl ₄	100	0.004	0.121	0.159	0.178	0.241	1.483	0.239
toluene	C ₆ H ₅ CH ₃	100	0.116	0.452	0.794	1.141	1.453	8.232	1.416
			<						
α -pinene	C ₆ H ₇ (CH ₃)(C(CH ₃)CH ₃)	100	0.001	0.123	0.163	0.177	0.214	0.841	0.211
α -thujene	CH ₂ CHC(CH ₃)CHC(CH ₂)(CHCH ₃ CH ₃)	100	0.005	0.092	0.116	0.135	0.172	0.538	0.158
			<						
β -ocimene	CH ₃ C(CH ₃)C ₃ H ₄ (CH ₃)C ₂ H ₃	94	0.001	< LOD	0.022	0.025	0.032	0.112	0.029
β -pinene	C ₆ H ₆ (CH ₂)(CH ₃) ₂	100	0.007	0.028	0.040	0.050	0.061	0.273	0.059

Table S5- concentration distribution information ($\mu\text{g}/\text{m}^3$) along with detection frequencies and limit of detection (LOD) values for MAU's indoor data.

species	Chemical formula	availability frequency (%)	LOD (ng)	min ($\mu\text{g}/\text{m}^3$)	1 st quartile ($\mu\text{g}/\text{m}^3$)	median ($\mu\text{g}/\text{m}^3$)	3 rd quartile ($\mu\text{g}/\text{m}^3$)	max ($\mu\text{g}/\text{m}^3$)	mean ($\mu\text{g}/\text{m}^3$)
1-butanol	C ₄ H ₉ OH	98	0.198	0.973	1.500	2.039	2.630	5.148	2.242
			<						
1-phenoxy-2-propanol	C ₆ H ₅ OCH(OH)CH ₃	59	0.001	< LOD	< LOD	0.007	0.017	0.036	0.010
1,2,4-trimethylbenzene	C ₆ H ₃ (CH ₃) ₃	93	0.004	< LOD	0.029	0.033	0.048	0.093	0.039
2-methyldecane	C ₁₁ H ₂₄	100	0.011	0.057	0.135	0.189	0.310	1.079	0.288
2-methylheptane	C ₈ H ₁₈	23	0.371	< LOD	< LOD	< LOD	< LOD	0.536	0.000
2-methylnonane	C ₁₀ H ₂₂	89	0.004	< LOD	0.074	0.094	0.142	0.432	0.114
2-methyloctane	C ₉ H ₂₀	100	0.006	0.167	0.214	0.265	0.330	0.506	0.283
3-carene	C ₆ H ₇ (CH ₃)(C(CH ₃)CH ₃)	31	0.011	< LOD	0.012	0.030	0.051	0.171	0.046
<i>n</i> -butyl acetate	CH ₃ CO ₂ (CH ₂) ₃ CH ₃	100	0.098	0.098	0.643	0.821	1.165	5.800	1.089
	C ₁₄ H ₂₈		<						
C13 cycloalkanes		97	LOD	< LOD	0.122	0.132	0.145	0.198	0.135
camphene	C ₆ H ₆ (CH ₃) ₂ (CH ₂)	98	0.014	< LOD	0.053	0.071	0.103	0.143	0.077
camphor	C ₅ H ₇ O(CH ₃)(C(CH ₃)CH ₃)	74	0.007	< LOD	0.125	0.177	0.283	0.461	0.203
<i>D</i> -limonene	C ₆ H ₈ (CH ₃)(C(CH ₃)CH ₂)	100	0.004	0.221	2.540	3.237	4.383	7.681	3.452
decamethylcyclopentasiloxane (D5)	Si ₅ O ₅ (CH ₃) ₁₀	100	0.046	0.229	2.347	3.613	4.779	8.506	3.636
	CH ₃ CH ₂ OH		<						
ethanol		100	0.001	0.903	3.903	5.550	7.153	12.321	5.638
	CH ₃ CO ₂ CH ₂ CH ₃		<						
ethyl acetate		100	0.001	0.130	2.516	3.234	5.172	17.130	4.163
ethylbenzene	C ₆ H ₅ CH ₂ CH ₃	95	0.085	< LOD	0.226	0.305	0.441	0.748	0.345
ethylene glycol monobutyl ether (EGBE)	CH ₃ CH ₂ CH ₂ CH ₂ - OC ₂ H ₄ OH	97	0.054	< LOD	0.279	0.377	0.636	1.465	0.479

ethylene glycol monoethyl ether (EGEE)	CH ₃ CH ₂ OCH ₂ CH ₂ OH	100	0.004	0.035	0.784	1.540	3.326	12.144	2.187
eucalyptol	C ₆ H ₁₀ (CH ₃)(OC(CH ₃)CH ₃)	93	0.004	< LOD	0.174	0.236	0.456	14.557	1.193
isopropanol	(CH ₃) ₂ CHOH	100	1.071	0.000	6.993	15.802	25.907	37.645	16.809
isopropylcyclohexane	C ₆ H ₁₁ (CHCH ₃ CH ₃)	100	0.001	0.104	0.157	0.178	0.198	0.290	0.182
<i>m</i> & <i>p</i> -xylene	(CH ₃) ₂ C ₆ H ₄	100	0.016	0.115	0.442	0.616	1.059	2.131	0.797
methyl acetate	CH ₃ COOCH ₃	44	0.057	< LOD	< LOD	< LOD	0.327	0.600	0.162
methyl ethyl ketone (MEK)	CH ₃ C(O)CH ₂ CH ₃	98	0.331	< LOD	1.581	1.862	2.309	4.754	2.033
methyl isobutyl ketone (MIBK)	(CH ₃) ₂ CHCH ₂ C(O)CH ₃	98	0.067	< LOD	0.709	0.830	1.227	5.425	1.104
<i>n</i> -decane	C ₁₀ H ₂₂	> 99	0.108	< LOD	0.245	0.389	2.961	14.247	1.938
<i>n</i> -dodecane	C ₁₂ H ₂₆	> 99	0.035	< LOD	0.119	0.166	0.242	0.924	0.208
<i>n</i> -heptane	C ₇ H ₁₆	100	0.098	0.195	2.359	2.930	3.793	7.931	3.429
<i>n</i> -hexane	C ₆ H ₁₄	100	0.065	0.349	1.042	1.353	1.873	3.362	1.466
<i>n</i> -nonane	C ₉ H ₂₀	100	0.018	0.132	0.316	0.465	0.690	1.338	0.515
<i>n</i> -octane	C ₈ H ₁₈	100	0.017	0.180	0.723	1.095	1.548	3.364	1.246
<i>n</i> -tetradecane	C ₁₄ H ₃₀	75	0.020	< LOD	0.098	0.128	0.159	0.344	0.138
<i>n</i> -tridecane	C ₁₃ H ₂₈	93	0.026	< LOD	0.051	0.065	0.082	0.203	0.068
<i>n</i> -undecane	C ₁₁ H ₂₄	85	0.118	< LOD	0.227	0.317	0.587	2.809	0.530
<i>o</i> -xylene	(CH ₃) ₂ C ₆ H ₄	100	0.009	0.107	0.232	0.295	0.425	0.741	0.338
octamethylcyclotetrasiloxane (D4)	Si ₄ O ₄ (CH ₃) ₈	100	0.031	0.080	0.178	0.259	0.375	6.974	0.509
phenoxyethanol	C ₆ H ₅ OC ₂ H ₄ OH	84	0.006	< LOD	< LOD	0.010	0.022	0.057	0.013
propylene glycol	CH ₃ CH(OH)CH ₂ OH	89	0.018	< LOD	0.479	0.633	0.871	1.832	0.711
tetrachloroethylene	C ₂ Cl ₄	100	0.004	0.112	0.192	0.217	0.280	0.782	0.252
toluene	C ₆ H ₅ CH ₃	100	0.116	0.120	1.121	1.475	2.617	6.322	2.001
α -pinene	C ₆ H ₇ (CH ₃)(C(CH ₃)CH ₃)	100	0.000	0.134	0.556	0.643	0.908	2.566	0.775
α -thujene	CH ₂ CHC(CH ₃)CHC(CH ₃)(CHCH ₃ CH ₃)	100	0.005	0.080	0.131	0.141	0.161	0.209	0.146
β -ocimene	CH ₃ C(CH ₃)C ₃ H ₄ (CH ₃)C ₂ H ₃	100	0.000	0.021	0.103	0.133	0.167	0.347	0.140
β -pinene	C ₆ H ₆ (CH ₂)(CH ₃) ₂	100	0.007	0.038	0.303	0.402	0.497	1.109	0.450

S4 VCP emissions in association with the sampling results

S4.1 Primary VCP sources associated with detected species

VCPs have remarkable overlap with the indoor sources that cause concentration enhancements in the MAU's exhaust stream. The emissions from building construction material originate primarily from paints, coatings, and adhesives. Furthermore, an essential portion of emissions from indoor activities like cleaning and using personal care products are related to VCPs. Thus, identifying the contribution of various VCP classes to emissions of the species selected for targeted analysis is insightful in source apportionment discussions. Table S6 includes the list of species considered in this study along with the major VCP sources, both indoor and outdoor, contributing to their emissions. These values are based on the Toronto VCP emissions estimated by Askari and Chan.⁵

Table S6- major VCP sources, located indoors and outdoors, for the species characterized in this study based on the Toronto data from the Canadian VCP emission inventory developed by Askari and Chan.⁵

species	Chemical formula	major indoor VCP source(s) ^d	major outdoor VCP source(s)
1-butanol	C ₄ H ₉ OH	coatings: > 80%	coatings: ≈ 100%
1-phenoxy-2-propanol	C ₆ H ₅ OCH(OH)CH ₃	cleaners: > 80%	cleaners: > 70% coatings: ≈ 10%
2-methyldecane	C ₁₁ H ₂₄	printing: ≈ 100%	--
2-methylheptane	C ₈ H ₁₈	cleaners: ≈ 90%	cleaners: ≈ 55% adhesives: ≈ 35%
2-methylnonane	C ₁₀ H ₂₂	printing: > 90% coatings: ≈ 2%	pesticides: ≈ 70% coatings: > 25%
2-methyloctane	C ₉ H ₂₀	printing: > 90% cleaners: ≈ 7%	adhesives: > 60% coatings: > 5%
C13 cycloalkanes	C ₁₄ H ₂₈	coatings: > 85%	pesticides: > 70% coatings: > 25%
cyclohexane	C ₆ H ₁₂	printing: ≈ 50% coatings: ≈ 50%	coatings: > 99%
<i>D</i> -limonene	C ₆ H ₈ (CH ₃)(C(CH ₃)CH ₂)	cleaners: ≈ 100%	cleaners: > 90%
decamethylcyclopentasiloxane (D5) ^a	Si ₅ O ₅ (CH ₃) ₁₀	personal care products: ≈ 100%	personal care products: ≈ 100%
ethyl acetate	CH ₃ CO ₂ CH ₂ CH ₃	printing: > 96% coatings: > 3%	coatings: ≈ 100%
ethanol	CH ₃ CH ₂ OH	cleaners: > 35% printing: > 30% personal care products: > 25%	cleaners: > 50% coatings: > 45%
ethylbenzene	C ₆ H ₅ CH ₂ CH ₃	printing: ≈ 70% coatings: ≈ 30% cleaners: > 99%	coatings: ≈ 100%
ethylene glycol monobutyl ether (EGBE)	CH ₃ CH ₂ CH ₂ CH ₂ -OC ₂ H ₄ OH	cleaners: > 99%	coatings: > 98%
ethylene glycol monoethyl ether (EGEE) fragrances ^b	CH ₃ CH ₂ OCH ₂ CH ₂ OH	coatings: ≈ 100% personal care products: ≈ 60% cleaners: ≈ 40%	coatings: ≈ 100% personal care products: > 75% cleaners: ≈ 20%
isopropanol	(CH ₃) ₂ CHOH	printing: > 65% personal care products: > 15% cleaners: > 10%	coatings: > 70% pesticides: > 17%
isopropylcyclohexane <i>m</i> & <i>p</i> -xylene	C ₆ H ₁₁ (CHCH ₃ CH ₃) (CH ₃) ₂ C ₆ H ₄	printing: ≈ 100% printing: > 96%	-- cleaners: > 50%

methyl acetate	$\text{CH}_3\text{COOCH}_3$	cleaners: >2%	coatings: > 45%
methyl ethyl ketone (MEK)	$\text{CH}_3\text{C(O)CH}_2\text{CH}_3$	coatings: \approx 100%	coatings: > 99%
		printing: > 85%	adhesives: > 60%
methyl isobutyl ketone (MIBK)	$(\text{CH}_3)_2\text{CHCH}_2\text{C(O)CH}_3$	coatings: \approx 15%	coatings: \approx 40%
		coatings: > 99%	coatings: > 79%
<i>n</i> -butyl acetate	$\text{CH}_3\text{CO}_2(\text{CH}_2)_3\text{CH}_3$	coatings: > 60%	adhesives: \approx 21%
		printing: \approx 40%	coatings: \approx 100%
<i>n</i> -decane	$\text{C}_{10}\text{H}_{22}$	coatings: > 85%	coatings: > 50%
<i>n</i> -dodecane	$\text{C}_{12}\text{H}_{26}$	coatings: > 85%	pesticides: \approx 50%
<i>n</i> -heptane	C_7H_{16}	coatings: > 85%	coatings: > 50%
<i>n</i> -hexane	C_6H_{14}	coatings: > 96%	pesticides: \approx 50%
			coatings: > 98%
<i>n</i> -nonane	C_9H_{20}	printing: > 98%	coatings: > 60%
		cleaners: \approx 1%	adhesives: > 35%
<i>n</i> -octane	C_8H_{18}	cleaners: > 50%	coatings: > 75%
		coatings: \approx 40%	adhesives: > 15%
<i>n</i> -pentadecane	$\text{C}_{15}\text{H}_{32}$	personal care products: > 75%	coatings: > 98%
		pesticides: > 20%	adhesives: > 15%
<i>n</i> -tetradecane	$\text{C}_{14}\text{H}_{30}$	personal care products: > 75%	coatings: > 98%
		pesticides: > 20%	coatings: > 98%
<i>n</i> -tridecane	$\text{C}_{13}\text{H}_{28}$	personal care products: > 75%	pesticides: > 90%
		pesticides: > 20%	pesticides: > 90%
<i>n</i> -undecane	$\text{C}_{11}\text{H}_{24}$	coatings: > 70%	pesticides: > 65%
		cleaners: > 15%	coatings: > 30%
<i>o</i> -xylene	$(\text{CH}_3)_2\text{C}_6\text{H}_4$	coatings: > 85%	coatings: > 50%
		printing: \approx 80%	pesticides: > 45%
octamethylcyclotetrasiloxane (D4)	$\text{Si}_4\text{O}_4(\text{CH}_3)_8$	coatings: > 15%	coatings: > 99%
		coatings: \approx 45%	coatings: \approx 100%
tetrachloroethylene	C_2Cl_4	adhesives: \approx 40%	coatings: \approx 100%
phenoxyethanol	$\text{C}_6\text{H}_5\text{OC}_2\text{H}_4\text{OH}$	coatings: > 90%	coatings: > 80%
		cleaners: > 80%	--
propylene glycol	$\text{CH}_3\text{CH(OH)CH}_2\text{OH}$	personal care products: > 15%	pesticides: > 85%
		personal care products: > 90%	pesticides: > 85%
toluene	$\text{C}_6\text{H}_5\text{CH}_3$	coatings: \approx 90%	coatings: > 90%
trimethylbenzenes ^c	$\text{C}_6\text{H}_3(\text{CH}_3)_3$	printing: > 90%	coatings: > 90%
		coatings: > 5%	

^a The original VCP emission inventory does not include D5 as an individual compound. However, D5 is well-known as a personal care product emission tracer.^{6,7}

^b We assumed fragrances to be identical to monoterpenoids in this study.

^c Among the different isomers, only 1,2,4-trimethylbenzene was consistently detected during this study (See Table S1).

S4.2 Estimating VCP emissions from the sampling site building

Downscaling the total indoor VCP emissions in Toronto to the building where our measurements were conducted was primarily done by scaling the emissions based on the ratio of building occupancy (\sim 200 residents) and the total population of the Greater Toronto Area (\sim 7.0 x 10⁶ people). All indoor emissions from VCP subcategories related to agricultural pesticides, industrial coatings and adhesives, industrial degreasers, and heavy-duty surface cleaners were excluded from

the analysis. Since printing emissions are less relevant to residents, we assumed (10 ± 5) % of the downscaled emissions to occur within the residence of interest. Furthermore, as the coating and adhesive emissions from architectural and furniture sources are supposed to be intense only during the first hours of the VCP application⁸, we assumed (20 ± 10) % of emissions from these sources to take place within our sampling site. Household cleaner and personal care product emissions may vary depending on building occupancy during the day. Accordingly, we assumed (80 ± 20) % of such emissions to apply to the sampling site.

A Monte Carlo analysis was employed to determine VCP emissions from the building and their associated uncertainty. Truncated Normal distributions with mean and standard deviation values based on the specifications above were considered for each VCP category. The scenarios were combined using the SOBOL combination algorithm in MATLAB (MathWorks, USA), and the indoor emissions were predicted for several combinations. Our analysis showed that 1200 combinations produced a well-repeatable result of indoor VCP emission distributions (See Figure 7 of the main text).

S5 Building emissions influenced by indoor sources

S5.1 Indoor sinks strength compared to the air exchange rate

Our previous study demonstrated that indoor chemistry and air-to-surface partitioning can modify 3 to 10 % of indoor VCP emissions.⁵ This phenomenon occurs because indoor chemistry and partitioning are not often fast enough to compete with the air exchange rate, leaving the indoor emissions almost unaffected before their transfer to outdoors. In other words, the time scale associated with indoor chemistry and air-to-surface partitioning tends to be appreciably longer than the ventilation rate. Here, we discuss a timescale comparison between indoor chemical loss phenomena and air exchange rate. Assuming that indoor chemical loss occurs primarily via reaction with airborne hydroxyl radical or ozone, the reactive timescale (τ_{rxn}) is given by Equation S7.

$$\tau_{rxn} = \left(k_{OH}[OH]_{indoor} + k_{O_3}[O_3]_{indoor} \right)^{-1} \quad S7$$

In Equation S7, k_{OH} and $\frac{k_{O_3}}{cm^3}$ are bimolecular rate constants for reaction with hydroxyl radical and ozone, respectively ($\frac{molecule.s}{molecule}$). $[OH]_{indoor}$ and $[O_3]_{indoor}$ are indoor concentrations of hydroxyl radical and ozone respectively (cm^3). Equation S8 defines Φ_{rxn} as the dimensionless ratio between the reactive and ventilation timescales.

$$\Phi_{rxn} = \frac{\tau_{rxn}}{\tau_{AER}} = \frac{AER}{k_{OH}[OH]_{indoor} + k_{O_3}[O_3]_{indoor}} \quad S8$$

In Equation S8, AER is the air exchange rate (s^{-1}), and τ_{AER} is the timescale associated with ventilation. The more the value of Φ_{rxn} deviates higher than unity, the slower the reactive loss is evaluated to be compared to ventilation. Note the analysis above does not consider the effect of surface reactions.

We utilized experimental kinetic data for k_{OH} and k_{O_3} .⁹ The rate constant values were determined using the GEKCO-A predictor for cases of missing experimental data.¹⁰ The indoor hydroxyl molecule

radical concentration was assumed to be variable between 10^4 and 10^5 cm^3 . Indoor ozone was considered to be a fraction of outdoor levels (10 to 50% according to Nazaroff and Weschler¹¹). Outdoor ozone levels for NAPS air quality stations close to the sampling site show a variability range of 4 to 45 ppb from 6:00 am to 6:00 pm in 2021.¹² Table S7 shows the Φ_{rxn} variability range per the aforementioned parameter extremes. Φ_{rxn} is at least of the 10^1 order of magnitude for most of the species, except a few monoterpenoids. The lower bound of Φ_{rxn} for the exceptional monoterpenoids corresponds to extreme outdoor ozone levels and high indoor ozone penetration factor. Since there was no extreme ozone pollution episode during the sampling period, these condition are hardly applicable to our measurements. Thus, we considered indoor chemistry to be too slow to compete with air exchange rate.

Table S7- range of variability of Φ_{rxn} , as given by Equation S7 for the species analyzed in this study.

species	Chemical formula	Φ_{rxn}
ethanol	CH ₃ CH ₂ OH	4.48 x 10 ² - 4.48 x 10 ³
isopropanol	(CH ₃) ₂ CHOH	2.83 x 10 ² - 2.83 x 10 ³
methyl ethyl ketone (MEK)	CH ₃ C(O)CH ₂ CH ₃	1.30 x 10 ³ - 1.30 x 10 ⁴
ethyl acetate	CH ₃ CO ₂ CH ₂ CH ₃	7.97 x 10 ² - 7.97 x 10 ³
propylene glycol	CH ₃ CH(OH)CH ₂ OH	6.84 x 10 ¹ - 6.84 x 10 ²
ethylene glycol monobutyl ether (EGBE)	CH ₃ CH ₂ CH ₂ CH ₂ OC ₂ H ₄ OH	5.59 x 10 ¹ - 5.59 x 10 ²
<i>n</i> -undecane	C ₁₁ H ₂₄	1.17 x 10 ² - 1.17 x 10 ³
<i>n</i> -dodecane	C ₁₂ H ₂₆	1.09 x 10 ² - 1.09 x 10 ³
<i>n</i> -nonane	C ₉ H ₂₀	1.47 x 10 ² - 1.47 x 10 ³
2-methyloctane	C ₉ H ₂₀	1.42 x 10 ² - 1.42 x 10 ³
<i>n</i> -butyl acetate	CH ₃ CO ₂ (CH ₂) ₃ CH ₃	2.54 x 10 ² - 2.54 x 10 ³
toluene	C ₆ H ₅ CH ₃	2.57 x 10 ² - 2.57 x 10 ³
<i>n</i> -pentadecane	C ₁₅ H ₃₂	8.07 x 10 ¹ - 8.07 x 10 ²
tetrachloroethylene	C ₂ Cl ₄	8.98 x 10 ³ - 8.98 x 10 ⁴
<i>D</i> -limonene	C ₆ H ₈ (CH ₃)(C(CH ₃)CH ₂)	1.04 x 10 ⁰ - 3.76 x 10 ¹
<i>n</i> -octane	C ₈ H ₁₈	1.84 x 10 ² - 1.84 x 10 ³
2-methylnonane	C ₁₀ H ₂₂	1.36 x 10 ² - 1.36 x 10 ³
cyclohexane	C ₆ H ₁₂	2.10 x 10 ² - 2.10 x 10 ³
1-butanol	C ₄ H ₉ OH	1.70 x 10 ² - 1.70 x 10 ³
<i>n</i> -hexane	C ₆ H ₁₄	2.63 x 10 ² - 2.63 x 10 ³
methyl isobutyl ketone (MIBK)	(CH ₃) ₂ CHCH ₂ C(O)CH ₃	1.12 x 10 ² - 1.12 x 10 ³
dichloromethane	CH ₂ Cl ₂	3.21 x 10 ¹⁸ - 3.21 x 10 ¹⁹
2-methylheptane	C ₈ H ₁₈	1.85 x 10 ² - 1.85 x 10 ³
<i>n</i> -tetradecane	C ₁₄ H ₃₀	8.76 x 10 ¹ - 8.76 x 10 ²
<i>n</i> -decane	C ₁₀ H ₂₂	1.31 x 10 ² - 1.31 x 10 ³
<i>n</i> -heptane	C ₇ H ₁₆	2.20 x 10 ² - 2.20 x 10 ³
2-methyldecane	C ₁₁ H ₂₄	1.20 x 10 ² - 1.20 x 10 ³
<i>n</i> -tridecane	C ₁₃ H ₂₈	9.52 x 10 ¹ - 9.52 x 10 ²
ethylbenzene	C ₆ H ₅ CH ₂ CH ₃	2.24 x 10 ² - 2.24 x 10 ³
<i>m</i> & <i>p</i> -xylene	(CH ₃) ₂ C ₆ H ₄	6.27 x 10 ¹ - 6.27 x 10 ²
1,2,4-trimethylbenzene	C ₆ H ₃ (CH ₃) ₃	4.68 x 10 ¹ - 4.68 x 10 ²
<i>o</i> -xylene	(CH ₃) ₂ C ₆ H ₄	1.09 x 10 ² - 1.09 x 10 ³
isopropylcyclohexane	C ₆ H ₁₁ (CHCH ₃ CH ₃)	1.15 x 10 ² - 1.15 x 10 ³
1-phenoxy-2-propanol	C ₆ H ₅ OCH(OH)CH ₃	3.56 x 10 ¹ - 3.56 x 10 ²
methyl acetate	CH ₃ COOCH ₃	4.15 x 10 ³ - 4.15 x 10 ⁴

ethylene glycol monoethyl ether (RGEE)		$7.56 \times 10^1 - 7.56 \times 10^2$
C13 cycloalkanes	$C_{14}H_{28}$	$7.89 \times 10^1 - 7.89 \times 10^2$
phenoxyethanol	$C_6H_5OC_2H_4OH$	$4.63 \times 10^1 - 4.63 \times 10^2$
octamethylcyclotetrasiloxane (D4)	$Si_4O_4(CH_3)_8$	$1.42 \times 10^3 - 1.42 \times 10^4$
decamethylcyclopentasiloxane (D5)	$Si_5O_5(CH_3)_{10}$	$1.42 \times 10^3 - 1.42 \times 10^4$
α -thujene	$CH_2CHC(CH_3)CHC(CH_2)(CHCH_3CH_3)$	$2.68 \times 10^{-1} - 1.40 \times 10^1$
α -pinene	$C_6H_7(CH_3)(C(CH_3)CH_3)$	$1.85 \times 10^1 - 2.48 \times 10^2$
camphene	$C_6H_6(CH_3)_2(CH_2)$	$2.47 \times 10^1 - 2.65 \times 10^2$
β -pinene	$C_6H_6(CH_2)(CH_3)_2$	$9.88 \times 10^0 - 1.58 \times 10^2$
β -ocimene	$CH_3C(CH_3)C_3H_4(CH_3)C_2H_3$	$4.67 \times 10^{-1} - 1.90 \times 10^1$
eucalyptol	$C_6H_{10}(CH_3)(OC(CH_3)CH_3)$	$1.20 \times 10^2 - 1.28 \times 10^3$
3-carene	$C_6H_7(CH_3)(C(CH_3)CH_3)$	$4.00 \times 10^0 - 1.05 \times 10^2$
linalool	$C_2H_3C(CH_3)(OH)C_3H_5C(CH_3)CH_3$	$5.88 \times 10^{-1} - 2.50 \times 10^1$
camphor	$C_5H_7O(CH_3)(C(CH_3)CH_3)$	$3.12 \times 10^2 - 3.12 \times 10^3$

While indoor chemistry leads to permanent species loss, air-to-surface partitioning is a temporary sink in absence surface reactions and irreversible sorption to surface substrates.¹³ Partitioning from air to surfaces is often accompanied by reverse resuspension from indoor surfaces. The surfaces reach thermodynamic equilibrium when deposition to and resuspension from surfaces tie in rate. The octanol-air partitioning coefficient, which parametrizes species' air-to-surface partitioning tendency when the surface has a mainly organic composition, was evaluated for the targeted species using the method proposed by Xiao and Wania.¹⁴ All the values were between 10 and 10⁷. Weschler and Nazaroff showed that more than 95% of emissions remain airborne for species associated with the range above, even when the surface concentrations reach their maximum values equivalent to equilibrium concentrations.¹⁵ Hence, air-to-surface partitioning loss can also be assumed to be negligible compared to the air exchange rate.

S5.2 MAU material and energy balance

Indoor-to-outdoor transfer rates were calculated using the MAU inlet and exhaust stream flow rates. The design values of stream flow rates were taken from the manufacturing company. The ventilation system had been assessed four times, within six-month periods, before our sampling date. The assessment reports showed a minimal deviation of measured flow rates from design values indicating that the nominal volumetric flow rates of exhaust and inlet streams from the MAU under which our air samples were collected were about 6500 and 4600 ft³/min, respectively. The other MAU's exhaust and inlet stream volumetric flow rates were about 8200 and 7600 ft³/min, respectively. Since we calculated concentrations as Normal values (See Equation S5), MAU's air stream densities were evaluated using the ideal gas law at T = 20°C and P = 1 atm. These calculations indicated that the MAUs make about 19800 kg/m³ of air to flow through the building, equivalent to about 16200 m³/h (9500 ft³/min). The building has 110 units with floor areas typically variable within 900 ± 100 ft². We assumed the typical wall height to be 8 ft and calculated the total volume associated with units. The resulting estimation was upscaled by 40% to account for indoor spaces within the building other than the units. Thus, the building's indoor space size was estimated to be (1.1 ± 0.1) × 10⁶ ft³. This estimation is comparable with the 1.7 × 10⁶ ft³ of the rectangular cuboid encompassing the whole building. Note that this rough analysis does not directly account for the indoor space occupied by objects displacing the air. The total indoor volume compared with the MAUs air handing capacity leads to a total building air exchange rate of about 0.52 h⁻¹, equivalent to an indoor residence time of about 115 minutes. In other words, the species detected on the exhaust stream are on average related to indoor emissions about two hours before the detection time. Accordingly, the indoor-outdoor comparison to find the ratios

and correlations (See Figure 8 of the main text) was conducted between each indoor series and the inlet data associated with two hours earlier. For example, the 10:00 am to 12:00 pm exhaust data were compared to 8:00 am to 10:00 am inlet numbers.

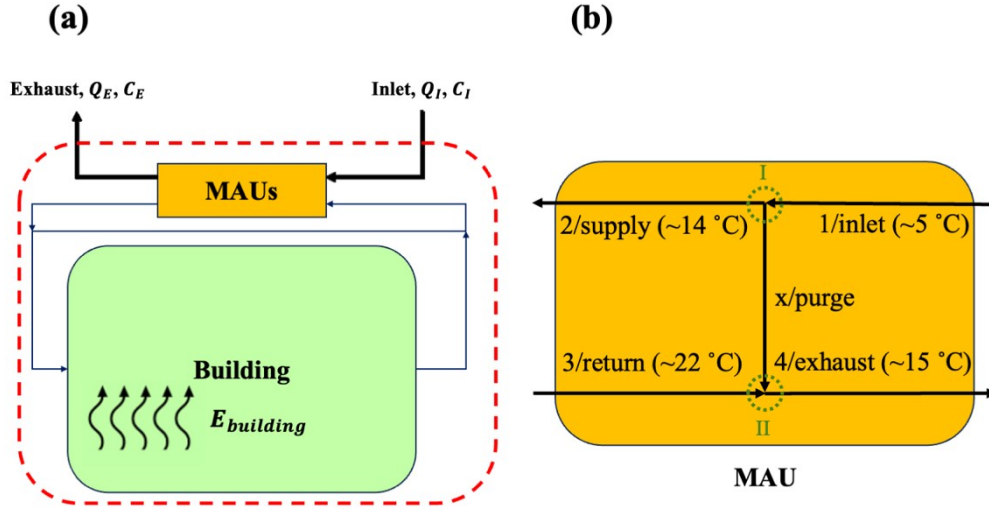


Figure S4- (a) a schematic diagram of the airflows through the mechanical ventilation system and the whole building in addition to (b) air streams associated with the MAU.

Figure S4(a) shows a schematic of the airflows within the building and its mechanical ventilation system. The MAUs add some makeup fresh air to the building's air recirculation system. A steady-state material balance for the control volume encompassing the building, the MAUs, and the recirculation path leads to Equation S9.

$$\Gamma \times (Q_I C_I - Q_E C_E) + E_{building} - L_{building} = 0 \quad S9$$

In Equation S9, $Q_I = 12200 \text{ ft}^3/\text{min}$ and $Q_E = 14700 \text{ ft}^3/\text{min}$ are MAU's total indoor and exhaust Normal volumetric flow rates. $E_{building}$ and $L_{building}$ are indoor gaseous emissions and permanent losses ($\mu\text{g}/\text{h}$), respectively. C_E and C_I are species Normal concentrations ($\mu\text{g}/\text{m}^3$) of the MAU's exhaust and inlet streams, respectively. Γ is the conversion factor from ft^3/min to m^3/h . As it was discussed in Section S5.1, the indoor permanent sinks are not expected to impact the indoor mass balance appreciably. Thus, assuming $L_{building} \approx 0$, Equation S9 simplifies to Equation S10 to estimate indoor emissions $E_{building}$ (See Figure 7 of the main text). Note that we only considered the data series leading to $Q_E C_E - Q_I C_I > 0$ to evaluate $E_{building}$ from Equation S10.

$$E_{building} \approx \Gamma \times (Q_E C_E - Q_I C_I) \quad S10$$

Since the return air is mixed with a fraction of the inlet stream, known as the purge flow, to yield the MAU's exhaust stream, the exhaust concentrations do not genuinely reflect the indoor effective concentrations. To calculate the indoor concentrations, one must consider the material balance of

air streams connected to an MAU. The total air mass balances for nodes *I* and *II* in Figure S4(b) lead to Equation S11 and Equation S12.

$$\dot{m}_1 = \dot{m}_x + \dot{m}_2 \quad \text{S11}$$

$$\dot{m}_4 = \dot{m}_x + \dot{m}_3 \quad \text{S12}$$

\dot{m} in Equation S11 and Equation S12 refers to the air stream mass flow rate ($\mu\text{g}/\text{h}$). The subscripts in Equations S11 and Equation S12 follow the fluid stream tags in Figure S4(b). There are three unknowns in Equation S11 and Equation S12: \dot{m}_2 , \dot{m}_3 , and \dot{m}_x . This condition requires an extra equation to determine the unknowns. A steady-state, ideal gas energy balance for the whole MAU leads to Equation S13 upon rearrangement.

$$\dot{m}_2 \bar{C}_{p_{1,2}} (T_1 - T_2) + \dot{m}_3 \bar{C}_{p_{3,4}} (T_3 - T_4) + \dot{m}_x \bar{C}_{p_{1,4}} (T_1 - T_4) \approx \dot{Q} \quad \text{S13}$$

In Equation S13, T_i denotes the temperature of stream *i* ($i = 1, 2, 3, 4$). $\bar{C}_{p_{i,j}}$ refers to the average air specific heat for streams *i* and *j*. $\dot{Q} = 14.8 \text{ MJ}/\text{h}$ is the heat transfer rate from the natural gas heater that warms up the supply stream to bring it to about 14°C. The three unknown mass flow rates mentioned above are determined by simultaneously solving Equation S11 to Equation S13, leading to $\dot{m}_2 \approx 7300 \text{ kg}/\text{h}$, $\dot{m}_3 \approx 9000 \text{ kg}/\text{h}$, and $\dot{m}_x \approx 1000 \text{ kg}/\text{h}$. The species material balance for node *II* in Figure S4(b) yields to Equation S14.

$$\frac{\dot{m}_3}{\rho_3} C_{indoor} + \frac{\dot{m}_x}{\rho_x} C_x = \frac{\dot{m}_4}{\rho_4} C_E \quad \text{S14}$$

In Equation S14, ρ denotes the gas stream density ($\mu\text{g}/\text{m}^3$). Note that $C_x = C_1 = C_I$ as stream *x* is a branch of the inlet stream. The indoor effective concentration (See Figure 8 of the main text) is determined by solving Equation S14 for C_{indoor} .

S6 Source apportionment analysis

A principal component analysis (PCA) technique was utilized to illustrate the primary emission sources driving the concentration profiles determined from sampling results (See Section S3). The quantified concentrations were arranged in a matrix with rows associated with individual sample series (e.g., an air sample collected on February 16 between 12:00 to 2:00 p.m.) and columns corresponding to individual chemical species. After arranging the data for inlet and exhaust concentrations, the respective matrices were input into the PCA algorithm. Only species with at least 80% of detection frequency were considered for the PCA. Our quality assurance runs showed that isopropanol tends to coelute from the GC column with normal pentane and acetone. Thus, although isopropanol's detection frequency was high enough for the PCA, it was excluded from the analysis to avoid interference from unquantified species.

The MATLAB software (MathWorks, USA) was used to conduct the PCA analysis. The software receives the data matrix described above and yields PCA loadings, scores, and the fraction of total

data variability grasped by the principal components, among other information. The loadings output from MATLAB are standardized to values within the [-1,1] interval. We kept this format of loadings representation for Figure 5 and Figure 6 of the main text as well as Figure S5 and Figure S6.

Table S8 and Table S9 show the data variability coverage for the principal components (PCs) associated with the MAU's exhaust and inlet streams, respectively. The first two PCs for the inlet data and the first three for the exhaust data are discussed in the main text (See Figure 5 and Figure 6 of the main text). Below is a discussion of the other important PCs for the MAU's air stream data.

Table S8- list of principal components associated with the MAU's exhaust stream along with their fraction of data variability coverage.

principal component #	% of data variability covered
1	40
2	18
3	12
4	10
5	8

Table S9- list of principal components associated with the MAU's inlet stream along with their fraction of data variability coverage.

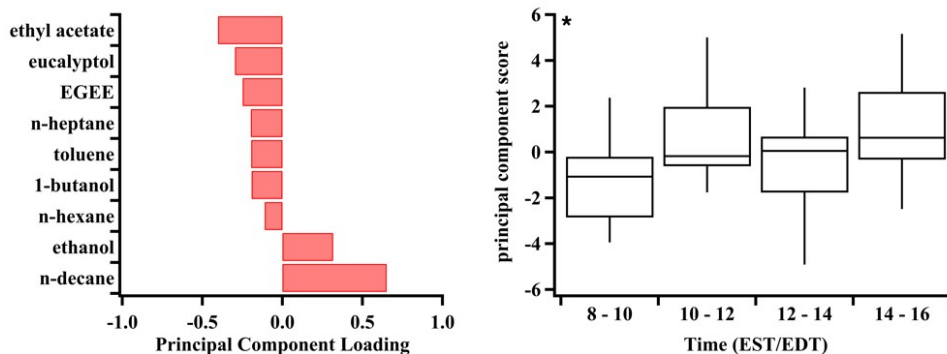
principal component #	% of data variability covered
1	63
2	17
3	9
4	5

Figure S5(a) shows the PCA results for the exhaust data's fourth PC. The PC is negatively loaded with traffic- and coating-related species like toluene, 1-butanol, and EGEE. On the other hand, the PC has positive loadings of *n*-decane and ethanol. The Canadian VCP emission inventory developed during an earlier study shows that about 8% of *n*-decane indoor VCP emissions are related to cleaners.⁵ Since ethanol is also associated with cleaners and the PC scores demonstrates significant diurnal variability, we consider this PC to be also related to cleaners in addition to the other cleaner-related PCs discussed in the main text. Figure S5(a) shows that the PC scores are typically lower during the 8:00 to 10:00 am interval. Further scrutinization revealed that the higher scores were pertaining to weekend data. Therefore, the PC may be related to cleaning activities generally less practiced during the weekday mornings.

Figure S5(b) shows the PCA results for the exhaust data's fifth PC. The PC score shows no significant diurnal variability. It also has positive loadings of coating-related species, such as EGEE, MEK, and *n*-heptane. Ethanol has the highest loading for this PC. While less than 3% of ethanol indoor emissions are related to coatings⁵, coatings account for more than 45% of outdoor ethanol emissions (See Table S6). Although outdoor coating emissions, impacted by industrial sectors, may show some diurnal variability, this effect is not observable in the PC score. Thus,

considering that this PC accounts for less than 10% of data variability, making deterministic explanations less viable, we designate this PC as another coating-related component, notwithstanding the complications of the contribution from ethanol emissions.

(a) Exhaust Stream 4th principal component



(b) Exhaust Stream 5th principal component

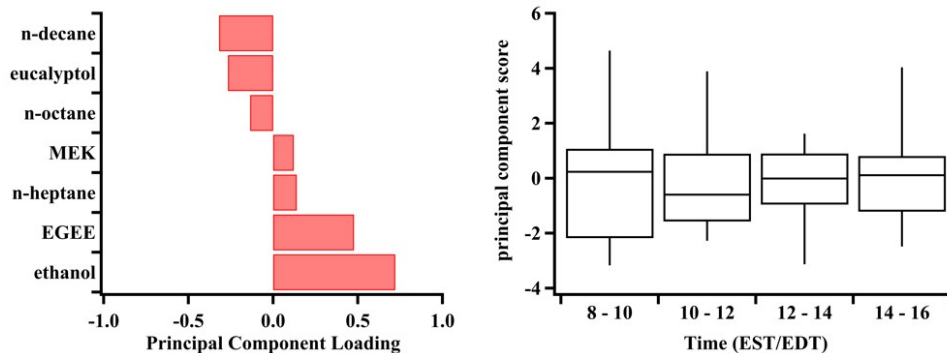


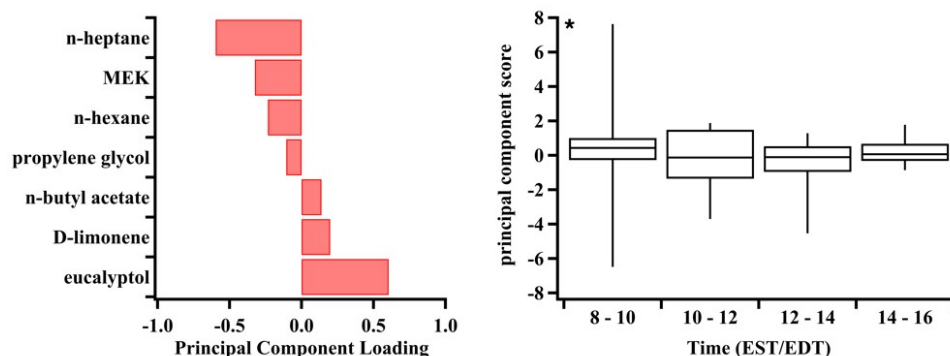
Figure S5- Principal component analysis (PCA) loading and score profiles for the fourth and fifth principal components (PCs) associated with exhaust data. PCA loadings are standardized to values within the $[-1,1]$ range. MEK and EGEE stand for methyl ethyl ketone and ethylene glycol monoethyl ether, respectively. The box plot whiskers on PCA score profiles correspond to score minima and maxima. An asterisk on the upper left corner of a score profile suggests a statistically significant ($p < 0.05$) PCA score diurnal variability. See Section S8 for details of statistical difference analysis.

Figure S6(a) shows the PCA results for the inlet data's third PC. The PC has higher positive loadings for D-limonene and eucalyptol, which are monoterpenoids likely coming from fragrances. The PC loading shows significant diurnal variability with extreme values during early morning, when personal care product emissions peak.⁸ Fragrance emissions mainly come from cleaners, but pesticides, coatings, and adhesives also contribute to outdoor fragrance emissions.⁵ Since the median scores in Figure S6(a) are relatively close and *n*-butyl acetate, mainly emitted from coatings (Table S6), has a positive loading, this PC may also minorly be impacted by outdoor steady VCP emissions. Thus, we assess this PC as mainly related to cleaning emissions with less intense influences from steady VCP sources.

Figure S6(b) includes PCA results for the fourth inlet data PC. This PC accounts for only 5% of data variability. The score profile shows significant enhancements during the mid-day. The loading profile is represented by some normal alkanes less related to daily-variable emissions (See Table S6). The mid-day increase may be related to cooking emissions. Our quality assurance tests

showed that the normal alkanes sometimes coelute with aldehydes during the GC analysis. Accordingly, the *n*-heptane, *n*-octane, and *n*-nonane detections may be partially influenced by pentanal, hexanal, and heptanal, respectively. These aldehydes are oxygenated species that may originate from cooking emissions.¹⁶ Therefore, this PC may be impacted by cooking activities during the mid-day, although it may represent other phenomena that are not straightforward to be identified given the minor variability fraction of inlet data explained by this PC.

(a) Inlet Stream 3rd principal component



(b) Inlet Stream 4th principal component

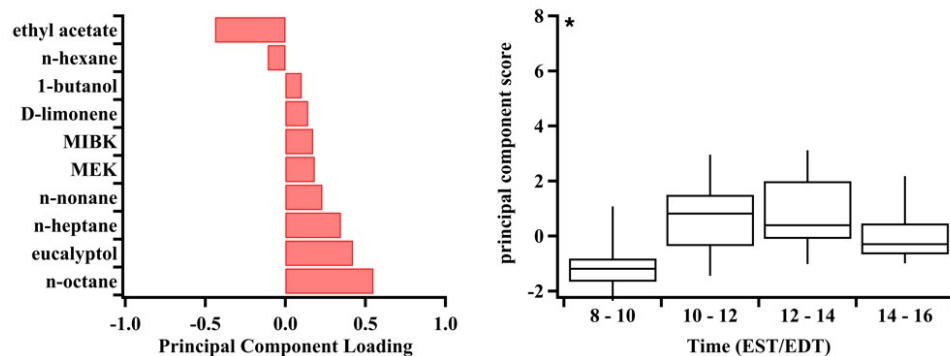


Figure S6- Principal component analysis (PCA) loading and score profiles for the third and fourth principal components (PCs) associated with inlet data. PCA loadings are standardized to values within the [-1,1] range. MEK and EGEE stand for methyl ethyl ketone and ethylene glycol monoethyl ether, respectively. The box plot whiskers on PCA score profiles correspond to score minima and maxima. An asterisk on the upper left corner of a score profile suggests a statistically significant ($p < 0.05$) PCA score diurnal variability. See Section S8 for details of statistical difference analysis.

S7 More discussion on the calculated indoor concentrations

Table S10 lists the detailed data on the ratio of indoor calculated indoor effective concentrations to ambient levels and their correlation. This data is a more extensive version of the numbers shown in Figure 8 of the main text.

Table S10- indoor-to-outdoor concentration ratio variability ranges and correlation coefficients for different time intervals. Missing data are due to lacking exhaust concentrations to calculate the effective indoor levels (See Equation S14). Correlation coefficients printed in bold are related to significant ($p < 0.05$) correlations.

species	Chemical formula	8:00 to 10:00 am outdoor versus 10:00 am to 12:00 pm indoor		10:00 am to 12:00 pm outdoor versus 12:00 to 2:00 pm indoor		12:00 to 2:00 pm outdoor versus 2:00 to 4:00 pm indoor	
		Indoor/Outdoor concentration ratio 5 th - 95 th percentile interval	Indoor- Outdoor correlation coefficient	Indoor/Outdoor concentration ratio 5 th - 95 th percentile interval	Indoor- Outdoor correlation coefficient	Indoor/Outdoor concentration ratio 5 th - 95 th percentile interval	Indoor- Outdoor correlation coefficient
1-butanol	C ₄ H ₉ OH	0.94 - 2.83	0.49	0.81 - 4.52	0.15	0.93 - 2.63	0.44
1-phenoxy-2-propanol	C ₆ H ₅ OCH(OH)CH ₃	0.05 - 1.17	0.21	0.23 - 5.11	0.22	0.24 - 4.66	-0.01
1,2,4-trimethylbenzene	C ₆ H ₃ (CH ₃) ₃	0.59 - 2.66	0.28	0.15 - 1.87	0.00	0.16 - 1.61	0.11
2-methyldecane	C ₁₁ H ₂₄	2.83 - 19.74	0.40	2.94 - 324.98	0.56	2.41 - 30.85	0.25
2-methylheptane	C ₈ H ₁₈	-	-	1.93 - 1.93	0.48	0.00 - 0.00	-0.19
2-methylnonane	C ₁₀ H ₂₂	0.71 - 4.82	0.18	0.64 - 3.93	-0.09	0.23 - 3.13	0.32
2-methyloctane	C ₉ H ₂₀	0.21 - 1.98	0.16	0.48 - 1.82	0.40	0.51 - 2.03	0.41
3-carene	C ₆ H ₇ (CH ₃)(C(CH ₃)CH ₃)	0.94 - 0.95	0.15	0.00 - 0.89	-0.30	0.08 - 3.40	-0.49
C13 cycloalkanes	C ₁₄ H ₂₈	0.36 - 1.37	0.04	0.36 - 1.67	-0.19	0.60 - 1.45	0.20
camphene	C ₆ H ₆ (CH ₃) ₂ (CH ₂)	0.85 - 3.20	-0.16	3.36 - 5.45	-0.30	2.13 - 5.65	-0.06
camphor	C ₅ H ₇ O(CH ₃)(C(CH ₃)CH ₃)	0.01 - 3.93	-0.13	0.17 - 6.43	0.37	0.03 - 3.39	0.20
<i>D</i> -limonene	C ₆ H ₈ (CH ₃)(C(CH ₃)CH ₂)	1.46 - 33.14	0.07	3.28 - 30.59	0.04	3.04 - 21.80	0.36
decamethylcyclopentasiloxane (D5)	Si ₅ O ₅ (CH ₃) ₁₀	1.81 - 29.11	0.38	2.94 - 45.70	-0.03	3.42 - 30.30	0.30
ethanol	CH ₃ CH ₂ OH	2.35 - 37.64	0.27	3.75 - 32.97	0.19	3.08 - 14.75	0.10
ethyl acetate	CH ₃ CO ₂ CH ₂ CH ₃	0.40 - 6.30	0.63	1.18 - 15.26	0.27	0.94 - 6.84	0.30
ethylbenzene	C ₆ H ₅ CH ₂ CH ₃	0.20 - 2.50	0.33	0.53 - 2.03	0.47	0.71 - 1.66	0.50
ethylene glycol monobutyl ether (EGBE)	CH ₃ CH ₂ CH ₂ CH ₂ - OC ₂ H ₄ OH	0.15 - 2.85	0.36	0.54 - 2.07	0.51	0.68 - 2.74	0.58
ethylene glycol monoethyl ether (EGEE)	CH ₃ CH ₂ OCH ₂ CH ₂ OH	0.17 - 1.24	0.57	0.14 - 1.47	0.26	0.20 - 0.97	0.53
eucalyptol	C ₆ H ₁₀ (CH ₃)(OC(CH ₃)CH ₃)	0.00 - 63.07	0.14	0.01 - 310.67	-0.02	0.10 - 12.84	0.22
isopropanol	(CH ₃) ₂ CHOH	0.19 - 28.85	-0.20	0.40 - 36.92	-0.12	0.26 - 34.51	-0.23
isopropylcyclohexane	C ₆ H ₁₁ (CHCH ₃ CH ₃)	0.52 - 1.79	0.06	0.58 - 1.87	0.16	0.76 - 2.03	0.30
linalool	C ₂ H ₃ C(CH ₃)(OH)C ₃ H ₅ C(CH ₃)CH ₃	0.00 - 3.06	0.26	0.11 - 4.86	0.33	1.10 - 7.16	-0.50
<i>m</i> & <i>p</i> -xylene	(CH ₃) ₂ C ₆ H ₄	0.65 - 3.58	0.48	0.55 - 3.25	0.46	0.75 - 2.35	0.59

methyl ethyl ketone (MEK)	$\text{CH}_3\text{C}(\text{O})\text{CH}_2\text{CH}_3$	0.60 - 1.86	0.26	0.38 - 2.81	0.12	0.43 - 1.77	0.20
methyl isobutyl ketone (MIBK)	$(\text{CH}_3)_2\text{CHCH}_2\text{C}(\text{O})\text{CH}_3$	0.45 - 1.45	0.42	0.43 - 2.20	0.29	0.41 - 1.90	0.32
<i>n</i> -butyl acetate	$\text{CH}_3\text{CO}_2(\text{CH}_2)_3\text{CH}_3$	0.49 - 2.95	0.48	0.84 - 5.88	0.44	0.89 - 3.04	0.52
<i>n</i> -decane	$\text{C}_{10}\text{H}_{22}$	2.22 - 55.26	0.46	1.12 - 67.76	0.03	1.58 - 52.56	0.25
<i>n</i> -dodecane	$\text{C}_{12}\text{H}_{26}$	2.01 - 13.62	0.40	2.49 - 31.34	0.25	2.29 - 12.69	0.41
<i>n</i> -heptane	C_7H_{16}	0.58 - 3.25	-0.05	0.40 - 2.99	0.09	0.33 - 1.97	0.15
<i>n</i> -hexane	C_6H_{14}	0.41 - 1.38	0.63	0.62 - 2.24	0.60	0.48 - 1.23	0.34
<i>n</i> -nonane	C_9H_{20}	0.73 - 3.71	0.15	0.30 - 2.73	0.19	0.31 - 2.69	0.10
<i>n</i> -octane	C_8H_{18}	0.46 - 3.80	0.04	0.23 - 2.77	0.01	0.19 - 3.20	-0.18
<i>n</i> -pentadecane	$\text{C}_{15}\text{H}_{32}$	0.40 - 4.37	0.24	0.25 - 2.47	0.13	0.12 - 4.90	-0.12
<i>n</i> -tetradecane	$\text{C}_{14}\text{H}_{30}$	1.77 - 805.23	-0.10	0.90 - 64.13	0.30	1.08 - 84.05	0.01
<i>n</i> -tridecane	$\text{C}_{13}\text{H}_{28}$	1.26 - 11.19	0.33	1.48 - 13.33	0.30	1.03 - 3.33	0.27
<i>n</i> -undecane	$\text{C}_{11}\text{H}_{24}$	0.97 - 77.40	0.31	1.19 - 235.76	0.36	0.62 - 19.19	0.05
<i>o</i> -xylene	$(\text{CH}_3)_2\text{C}_6\text{H}_4$	0.60 - 2.50	0.42	0.58 - 2.24	0.54	0.73 - 1.70	0.56
octamethylcyclotetrasiloxane (D4)	$\text{Si}_4\text{O}_4(\text{CH}_3)_8$	0.79 - 33.79	0.24	0.45 - 3.93	-0.08	0.63 - 14.98	0.16
phenoxyethanol	$\text{C}_6\text{H}_5\text{OC}_2\text{H}_4\text{OH}$	0.10 - 136.78	0.38	0.02 - 2.33	-0.14	0.52 - 3.49	0.40
propylene glycol	$\text{CH}_3\text{CH}(\text{OH})\text{CH}_2\text{OH}$	0.06 - 2.98	0.23	0.21 - 2.83	0.24	0.18 - 1.52	0.67
tetrachloroethylene	C_2Cl_4	0.39 - 1.50	0.29	0.61 - 1.97	0.35	0.66 - 1.52	0.47
toluene	$\text{C}_6\text{H}_5\text{CH}_3$	0.55 - 2.75	0.55	0.64 - 3.31	0.40	0.71 - 4.36	0.47
α -pinene	$\text{C}_6\text{H}_7(\text{CH}_3)(\text{C}(\text{CH}_3)\text{CH}_3)$	1.85 - 5.57	0.27	1.79 - 15.19	0.12	2.69 - 7.42	0.39
α -thujene	$\text{CH}_2\text{CHC}(\text{CH}_3)\text{CHC}(\text{CH}_2)(\text{CHCH}_3\text{C}$ $\text{H}_3)$	0.17 - 1.38	0.11	0.48 - 1.84	0.12	0.62 - 1.50	0.16
β -ocimene	$\text{CH}_3\text{C}(\text{CH}_3)\text{C}_3\text{H}_4(\text{CH}_3)\text{C}_2\text{H}_3$	1.81 - 7.36	0.32	3.17 - 7.75	0.30	3.66 - 7.89	0.59
β -pinene	$\text{C}_6\text{H}_6(\text{CH}_2)(\text{CH}_3)_2$	2.81 - 12.03	0.20	3.65 - 31.15	-0.04	5.50 - 15.85	0.39

In addition to the atmospheric effects of air pollution, gaseous organic emissions may be toxic. This study suggested that indoor gaseous pollutant concentrations are elevated within indoor spaces. Since people spend most of their time indoors, indoor exposure to air pollutants is increasingly becoming a more critical factor in public health. Table S11 shows the toxic thresholds for the species in Figure 8 of the main text, as given by the toxicology data in the PubChem online database.¹⁷ These toxicology data are pertaining to exposure via inhalation. Data in Table S11 are reported for humans or animals in case of lacking human studies.

Table S11- toxicology data for exposure to species shown in Figure 8 of the main text via inhalation.¹⁷ LDLo and TCLo refer to lowest lethal dose and lowest toxic concentration, respectively. LC50 is the dose lethal to half of the studies animals.

<i>n</i> -octane	C ₈ H ₁₈	acute effects mouse: LDLo = 80000 mg/kg of body weight over two hours rat: LC50 = 25250 ppm over four hours
methyl ethyl ketone (MEK)		reproductive effects mouse: 3000 ppm over seven hours rat: 1000-3000 ppm over seven hours acute effects human: TCLo = 100 ppm over five minutes human: TCLo = 10 ppm over four hours
decamethylcyclotetrasiloxane (D5)	Si ₅ O ₅ (CH ₃) ₁₀	acute effects rat: LC50 > 2700 mg/m ³ over four hours
<i>n</i> -heptane	C ₇ H ₁₆	acute effects human: TCLo = 1000 ppm over six minutes
methyl isobutyl ketone (MIBK)	(CH ₃) ₂ CHCH ₂ C(O)CH ₃	acute effects guinea pig: LC50 = 16800 ppm over six hours Note: The IARC has classified MIBK as a Group 2B (i.e., possibly carcinogenic to humans) compound.
butyl acetate	CH ₃ CO ₂ (CH ₂) ₃ CH ₃	reproductive effects rat: 1500 ppm over seven hours acute effects human: TCLo = 200 ppm
ethyl acetate	CH ₃ CO ₂ CH ₂ CH ₃	acute effects human: TCLo = 400 ppm
<i>n</i> -decane	C ₁₀ H ₂₂	acute effects rat: LC50 > 1369 ppm over eight hours mouse: LC50 = 72300 mg/m ³ over two hours
octamethylcyclotetrasiloxane (D4)	Si ₄ O ₄ (CH ₃) ₈	acute effects rat: LC50 = 36 g/m ³ over four

toluene	$C_6H_5CH_3$	hours mutagenic effects human: 252 $\mu\text{g/L}$ over nineteen years reproductive effects rat: 1500 mg/m^3 over four hours, 1000 mg/m^3 over twenty-four hours, 2000 ppm over six hours, 800 mg/m^3 over six hours, 1200 ppm over six hours mouse: 500 mg/m^3 over twenty-four hours, 1000 ppm over six hours, 200 ppm over seven hours acute effects human: TLo = 50 ppm, 750 mg/m^3 over eight hours, 200 ppm over fifteen minutes
<i>D</i> -limonene	$C_6H_8(CH_3)(C(CH_3)CH_2)$	mutagenic effects human: 1 mmol/L over forty-eight hours
1-butanol	C_4H_9OH	acute effects human: TLo = 25 ppm
ethanol	CH_3CH_2OH	acute effects human: TLo = 1800 ppm over thirty minutes, 2500 ppm over twenty minutes
ethylene glycol monoethyl ether (EGEE)	$CH_3CH_2OCH_2CH_2OH$	acute effects rat: LC50 = 2000 ppm over seven hours
<i>n</i> -hexane	C_6H_{14}	reproductive effects rat: 100-5000 ppm mouse: 200-5000 ppm

As the calculated effective indoor concentrations indexed in Table S5 show, even the maximum indoor concentrations are well below the toxic thresholds of Table S11. Thus, the indoor emissions in this study are more critical regarding their impact on ambient air quality than residents' near-field exposure. Nevertheless, indoor residents may still feel unpleasant symptoms from poor air quality levels associated with indoor concentrations below the toxic levels. Thus, indoor enhancements of air pollutants may still be critical for more intense indoor emissions and poor ventilation conditions.

S8 Proper statistical hypothesis tests to inspect significant trends across data

The appropriate statistical test was selected based on data normality, dependence, and symmetry considerations. Table S12 lists the suitable analysis types per those criteria.¹⁸ The tests suitable for Normal data were only used when both data series under comparison were determined to follow a Normal distribution. We used the Shapiro-Wilk test to assess for Normality. The Kendall correlation p-value was assessed to check for dependence. The data were assumed to be dependent if the correlation p-value was less than 0.05. We evaluated data symmetry by assuming data series with skewness absolute value below 0.5 to be un-skewed. Any data points deviating from the

median by more than three times of median absolute deviation (MAD) were assumed to be an outlier. Table S12 shows that variance parity is an extra factor to determine the appropriate test for normally-distributed data. This factor was analyzed using the two-sample F-test.

Table S12- The appropriate statistical hypothesis test for different categories of data normality, dependence, and symmetry.¹⁸

Appropriate test	conditions
Student's t-test	Normality: both series are normally distributed Dependence: the series are independent Symmetry: symmetric + no outliers Other conditions: similar variance
Welch's t-test	Normality: both series are normally distributed Dependence: the series are independent Symmetry: symmetric + no outliers Other conditions: unequal variance
Paired t-test	Normality: both series are normally distributed Dependence: the series are dependent Symmetry: symmetric + no outliers
Mann-Whitney U-test	Normality: no limitation Dependence: the series are independent Symmetry: no limitation
Wilcoxon signed-rank test	Normality: no limitation Dependence: the series are dependent Symmetry: no limitation

References

- (1) *Weather Historical Data*. https://climate.weather.gc.ca/historical_data/search_historic_data_e.html (accessed 2023-07-18).
- (2) Van Den Dool, H.; Kratz, P. D. A Generalization of the Retention Index System Including Linear Temperature Programmed Gas-Liquid Partition Chromatography. *J Chromatogr* **1963**, *11*, 463–471.
- (3) *NIST Chemistry WebBook*. <https://webbook.nist.gov/chemistry/> (accessed 2023-07-18).
- (4) Pankow, J. F.; Asher, W. E. Atmospheric Chemistry and Physics SIMPOL.1: A Simple Group Contribution Method for Predicting Vapor Pressures and Enthalpies of Vaporization of Multifunctional Organic Compounds. *Atmos Chem Phys* **2008**, *8*, 2773–2796. <https://doi.org/https://doi.org/10.5194/acp-8-2773-2008>.
- (5) Askari, A.; Chan, A. W. H. Organic Emissions of Volatile Chemical Products in Canada: Emission Inventories, Indoor-to-Outdoor Transfer, and Regional Impacts. *Environ Sci Technol* **2024**, *58* (25). <https://doi.org/10.1021/acs.est.3c10753>.

- (6) Gkatzelis, G. I.; Coggon, M. M.; McDonald, B. C.; Peischl, J.; Aikin, K. C.; Gilman, J. B.; Trainer, M.; Warneke, C. Identifying Volatile Chemical Product Tracer Compounds in U.S. Cities. *Environ Sci Technol* **2021**, *55* (1), 188–199. <https://doi.org/10.1021/acs.est.0c05467>.
- (7) Coggon, M. M.; McDonald, B. C.; Vlasenko, A.; Veres, P. R.; Bernard, F.; Koss, A. R.; Yuan, B.; Gilman, J. B.; Peischl, J.; Aikin, K. C.; Durant, J.; Warneke, C.; Li, S. M.; De Gouw, J. A. Diurnal Variability and Emission Pattern of Decamethylcyclopentasiloxane (D5) from the Application of Personal Care Products in Two North American Cities. *Environ Sci Technol* **2018**, *52* (10), 5610–5618. <https://doi.org/10.1021/acs.est.8b00506>.
- (8) Stockwell, C. E.; Coggon, M. M.; I. Gkatzelis, G.; Ortega, J.; McDonald, B. C.; Peischl, J.; Aikin, K.; Gilman, J. B.; Trainer, M.; Warneke, C. Volatile Organic Compound Emissions from Solvent-and Water-Borne Coatings-Compositional Differences and Tracer Compound Identifications. *Atmos Chem Phys* **2021**, *21* (8), 6005–6022. <https://doi.org/10.5194/acp-21-6005-2021>.
- (9) Atkinson, R.; Arey, J. Atmospheric Degradation of Volatile Organic Compounds. *Chem Rev* **2003**, *103* (12), 4605–4638. <https://doi.org/10.1021/CR0206420>.
- (10) GECKO-A : Generator for Explicit Chemistry and Kinetics of Organics in the Atmosphere. <http://geckoa.lisa.u-pec.fr/> (accessed 2022-03-08).
- (11) Nazaroff, W. W.; Weschler, C. J. Indoor Ozone: Concentrations and Influencing Factors. *Indoor Air*. John Wiley and Sons Inc January 1, 2022. <https://doi.org/10.1111/ina.12942>.
- (12) National Air Pollution Surveillance (NAPS) Program - Open Government Portal. <https://open.canada.ca/data/en/dataset/1b36a356-defd-4813-acea-47bc3abd859b> (accessed 2022-02-02).
- (13) Algrim, L. B.; Pagonis, D.; de Gouw, J. A.; Jimenez, J. L.; Ziemann, P. J. Measurements and Modeling of Absorptive Partitioning of Volatile Organic Compounds to Painted Surfaces. *Indoor Air* **2020**, *30* (4), 745–756. <https://doi.org/10.1111/ina.12654>.
- (14) Xiao, H.; Wania, F. Is Vapor Pressure or the Octanol–Air Partition Coefficient a Better Descriptor of the Partitioning between Gas Phase and Organic Matter? *Atmos Environ* **2003**, *37* (20), 2867–2878. [https://doi.org/10.1016/S1352-2310\(03\)00213-9](https://doi.org/10.1016/S1352-2310(03)00213-9).
- (15) Weschler, C. J.; Nazaroff, W. W. Semivolatile Organic Compounds in Indoor Environments. *Atmos Environ* **2008**, *42* (40), 9018–9040. <https://doi.org/10.1016/j.atmosenv.2008.09.052>.
- (16) Takhar, M.; Li, Y.; Ditto, J. C.; Chan, A. W. H. Formation Pathways of Aldehydes from Heated Cooking Oils. *Environ Sci Process Impacts* **2023**, *25*, 165–175. <https://doi.org/10.1039/d1em00532d>.
- (17) PubChem. <https://pubchem.ncbi.nlm.nih.gov/> (accessed 2023-07-18).
- (18) James, G.; Witten, D.; Hastie, T.; Tibshirani, R. *An Introduction to Statistical Learning: With Applications in R*, 1st ed.; Springer/Sci-Tech/Trade, 2021; Vol. 103.